CHAPTER 5

ELUCIDATING THE ROLE OF NATURAL ANTISENSE RNA LOCI AS PRO-SURVIVAL TO PRO-DEATH MOLECULAR SWITCH IN THE IRE1A SIGNALING PATHWAY IN ARABIDOPSIS THALIANA

by

Taiaba Afrin[1], Karolina M. Pajerowska-Mukhtar[1]
[1] Department of Biology, University of Alabama at Birmingham, 1300 University Blvd., Birmingham, AL 35294, USA

In eukaryotic cells, both biotic and abiotic stress can disrupt the proper functioning of the endoplasmic reticulum (ER), leading to a response known as the unfolded protein response (UPR). This response is aimed at mitigating ER stress and is initiated by a highly conserved UPR sensor called Inositol-Requiring Enzyme 1 (IRE1). IRE1 activates a pro-survival pathway to protect the cell. However, when the stress conditions become extreme or chronic, the cells undergoing UPR may switch from pro-survival to pro-death signaling to avoid unfavorable circumstances for the overall well-being of the organism. In plants, the specific mechanisms responsible for attenuating the pro-survival branch of IRE1a signaling are not yet well understood. In the model plant Arabidopsis, it has been observed that during ER stress, IRE1a directly cleaves the mRNA of a transcription factor called bZIP60 (basic leucine zipper 60). This cleavage leads to the production of an active form of bZIP60, which then activates genes involved in cellular protection. To investigate the regulatory mechanisms governing bZIP60 expression during the immune response in plants, we conducted a study using the plant bacterial pathogen *Pseudomonas syringae* pv. tomato (*Pst* DC3000) as a biotic inducer of ER stress. Our findings revealed the involvement of a novel microRNA called miR5658 in targeting bZIP60 for degradation. Further experiments using reporter-based assays confirmed that the binding sequence of miR5658 on bZIP60 mRNA was necessary for its degradation. Additionally, T-DNA mutants lacking miR5658 showed increased stability of bZIP60 transcript. Collectively, our results indicate that in response to triggering cell death stimuli, miR5658 target bZIP60 mRNA which effectively turns off the pro-survival pathway mediated by IRE1a, thereby tipping the scales towards a pro-death signaling cascade. These findings

stress and immune responses in plants.

Introduction

Because of plants autotrophic nature they are very appealing food source of many exploitive species like microbes, insects, animals [1]; their survival and health rely on their abilities to identify and imply appropriate defensive strategies against those exploitive species. Hence plants have evolved multilayer defense systems to thrive in nature. Unlike animals, plants have their unique innate immune system, where every single cell expresses innate immune receptors to identify invasion signals [2]. Plants have cell surface localized pattern recognition receptors (PRRs) to identify the pathogen/microbe-associated molecular pattern (PAMPs/MAMPs) or host-derived damage-associated molecular pattern (DAMPs) and execute defense responses [2,3]. The successful recognition leads towards pattern-triggered immunity (PTI), the very first line of defense responses of plants against almost all microbial pathogens [2,4,5]. Some pathogens evolved to encode effector molecules as pathogenic virulence to delay or impede and/or restrain PTI and result in effector triggered susceptibility (ETS). In contrast plants also evolved resistance (R) genes to specifically detect effectors, triggers a rapid and higher amplitude of defense responses leading to effector triggered immunity (ETI) [2,4,5]. The recognition of pathogen effectors by R genes triggers hypersensitive response (HR) most of the cases [4] through programmed cell death (PCD), production of reactive oxygen species (ROS), antimicrobial compound synthesis at the infected tissue [4,6,7]. For many instances there is no distinct difference in-between PTI and ETI [8] and ETI is referred to as amplified PTI [2]. Hence plant

employ defense responses [9]. Usually PTI mediated PCD appears after several days of infection, while ETI triggered HR PCD happens within hours of infection [7].

Among different phytohormones that modulate HR cell death under diverse environmental situations, salicylic acid (SA) is well described regulator of systemic acquired resistance (SAR) [10]. During immune response, endogenous SA serve crucial functions in controlling HR and cell death. Several studies confirmed that elevated levels of SA is required for establishment of local and systemic resistance [11]. Non-expressor of pathogenesis related gene 1 (NPR1) gene is the master regulator of defense gene expressions as well as plant immunity and highly conserved in plant species [12,13]. NPR1 transduce SA signaling through activating downstream PR genes and positively regulate SAR [14]. Following exposure to Salicylic Acid (SA), NPR1 has the capacity to stimulate its own expression [15], This triggers a co-regulatory mechanism where both transcription and post-transcriptional regulation of NPR1 come into play [11]. NPR proteins can regulate immunity by interacting with other hormone regulatory pathway as well as by reprogramming a huge gene expression networks [16]. NPR1 interacts with members of the basic leucine zipper transcription factor family to trigger defense responses after entering the nucleus [17].

Endoplasmic reticulum (ER) is an integral point for multiple cellular stress response pathways. In eukaryotic cells ER is known as protein folding machinery as it is the maturation site of secretory and membrane proteins. When the protein folding and assembly is perturbed in ER, the unfolded and misfolded protein accumulate in ER and cause ER stress. ER stress triggers response mechanisms termed as unfolded protein response (UPR) to maintain cellular homeostasis [18-20]. Among three different pathways

IRE1 is type-1 membrane protein. In plants *IRE1* mediates transcriptional activation of genes encoding ER chaperons and folding enzymes, through unconventional splicing of bZIP60 mRNA [22-25]. The spliced bZIP60 travels to nucleus, acts as transcription factor and activate cytoprotective genes [19,22,23,25]. *IRE1* can also mediate the bulk mRNA degradation to reduce the nascent protein load through the process regulated *IRE1*-dependent decay (RIDD) [24,26].

Throughout the course of evolution, plants have been subjected to extreme biotic and abiotic stress, which they have managed through intricate molecular mechanisms. These complex mechanisms evolved over time and helped plants to survive and sustain in extreme environmental condition. Non-protein coding DNA contribute equally to this complex adaptation process compared to protein coding DNA. The non-protein coding DNA (also known as "junk" DNA) transcribes a substantial amount of the transcriptional unit identified as non-coding RNAs (ncRNAs) and plays crucial functions in a variety of regulatory processes [27]. Long non coding RNA (lncRNA, >200 nucleotides) are a type of regulatory ncRNA [28]. Long noncoding natural antisense transcript (lncNAT), the lncRNA overlap with one or more exons of a different transcript on the opposite strand are one of the categories of ncRNA. The lncRNAs mode of action varies widely; they can interact with other genes, hormones, proteins, ncRNAs; act as precursor of miRNAs, siRNAs; act as target mimicry of other miRNAs; can be co-induce with other neighboring defensive genes [29-34]. Few recent studies are implicating the significant importance of lncRNA, lncNAT in plants defense response mechanisms [32,35].

are particularly found to involved with various abiotic and biotic stress response mechanisms in many species. For example, *Homo sapiens*, *Mus musculus*, *Saccharomyces cerevisiae*, *Plasmodium falciparum*, *Oryza*, *Zea mays*, *Triticum*, *Brassica rapa*, *Arabidopsis* [36-46]. lncNAT can regulate the expression level of sense transcript [47,48]. Depending on the nature of NATs effect on sense transcript, NATs can be categorized into two: concordant (NAT and sense transcripts expresses coordinately), discordant (NAT and sense transcript have opposite expression pattern) [36,49,50]. For example, the Arabidopsis cold-assisted intronic non-coding RNA (COOLAIR) represses the Flowering locus C (FLC) sense transcript by altering histone marks [50]; a cis-NAT in Rice boosts the translation of its cognate sense mRNA in order to maintain phosphate homeostasis and plant fitness [49]. Due to their wide range the general biological functions and regulatory mechanism are elusive. Researchers have demonstrated that NATs utilize variety of ways to regulate the transcriptional or post-transcriptional expression of sense transcripts for example, translation initiation [51], mRNA stability [52], transcription termination [53], DNA methylation [54], histone methylation [55], translational enhancement [49,56], RNA interference [57], gene silencing [58], RNA masking induced alternative splicing [59], RNA editing [60].

In plants many NATs are identified so far, i. e. 7-9% of all transcripts are overlapped as cis-NATs [40]. In Arabidopsis ~88% of cis-NATs pairs are paired as protein coding genes and non-protein coding transcripts [61]. These cis NATs may form a complex regulatory network, but the current understanding of their role and function is very limited. Several studies in model plant *Arabidopsis thaliana* found NAT's crucial involvement in developmental processes, for instance during germination [62], flowering [63] and

in different plants, i. e. in Arabidopsis during salt tolerance [45,46], cold acclimation [65]; in rice phosphate starvation [49] and leaf blade flattening [66], in tomato oomycete resistance [67]. Along with these direct function they can act as precursors of siRNA [45] and miRNA [68].

Plant miRNAs pair with their targets nearly-perfectly and can cause mRNA cleavage. miRNAs are small lncRNA with an average 22 nucleotide length. Most of the reported miRNA interact with their target mRNA at 3'UTR (untranslated region) [69], but also been reported to interact with 5' UTR, coding region and promotor region [70]. Through interaction miRNAs can suppress or activate gene expression depending on the condition [69,71]. Several recent articles proved the shuttling of miRNA into different subcellular compartment to control transcription and translation rate [72]. miRNAs can move from one cell to another through plasmodesmata and for systemic long distance through vasculature and can act as mobile signaling molecule [73,74]. miRNAs are not only mobile within the plant, but it can also move between plants and interacting organisms [75,76].

miRNAs have been reported to regulate plants developmental [77,78], biotic [79,80] and abiotic stress responses [81-86]. Several miRNAs have been reported in mammalian system intertwined with ER stress responsive pathway. For example, miR-211 has been reported as key regulator of PERK-ATF4 mediated pro-survival signaling during mammalian ER stress responses [87]. Few of them are reported to be involved in shaping the *IRE1α-XBP1* mediated pathway. miR-214 [88], miR-30-c-2* [89], miR-34c-5p [90], miR-665 [91] regulate *XBP1* expression under different circumstances; miR-1291 can directly target *IRE1α* within its 5'-UTR in hepatoma cells, leading to overexpression of the pro-oncogenic protein glypicn-3 [92].

kind of stress, but the involvement of miRNA in ER stress response mechanisms in plants particularly in Arabidopsis has not been investigated properly. In this study, we demonstrated the regulatory roles of novel miRNA miR5658 during the transition from pro-survival to pro-death molecular switch. Functional analysis indicated that miR5658 regulate cell death during acute ER stress (caused by *Pst* DC3000 avrRPM1) by controlling *bZIP60* expression. We also showed that the sense transcript of miR5658 precursor cis-NAT does not interfere during the cell death regulation, rather the sense transcript concordantly supports cis-NAT in this regulation. This finding provides insight into the function of cis-NATS in miRNA guided call death during acute ER stress.
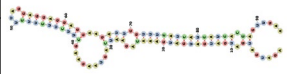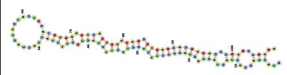
Results

Identification and analysis of novel miRNAs that can target bZIP60 transcript:

miRNAs are well established key regulators of different stress responsive mechanism in both mammalian and plant system. As there are already identified miRNAs that regulate the *IRE1α-XBP1* mediated pathway during ER stress, we sought to identify miRNAs that can regulate *IRE1a-bZIP60* mediated pathway in model plant *Arabidopsis thaliana*. To identify the miRNAs, which can target *bZIP60* (spliced or unspliced form), first we performed a prediction analysis using miRBase website (https://mirbase.org). By using sequence analysis of *bZIP60* and mature miRNAs, we have predicted three microRNAs that can target *bZIP60* (Table 1). We then confirmed the prediction using psRNATarget: A Plant small RNA Target Analysis Server (https://www.zhaolab.org/psRNA-Target/) website. Among them miR5658 and miR414 target *bZIP60* at exon 1, miR397b

(http://rna.tbi.univie.ac.at//cgi-bin/RNAWebSuite/RNAfold.cgi), the predicted secondary structures of microRNA's are presented in table 1.

Table 1: **Predicted miRNAs, which can target both spliced and unspliced bZIP60 transcript**. The prediction was performed using "miRBase: the microRNA database" (https://mirbase.org). E value, alignment and target location was adapted from the miRBase prediction. Secondary structure was predicted using "RNAfold WebServer" (http://rna.tbi.univie.ac.at//cgi-bin/RNAWebSuite/RNAfold.cgi).

microRNA ID	E Value	Predicted Secondary Structure	Alignment with bZIP60	Target Location
ath-miR5658	1.3		bzip60 388 a u g a u g a u g a u g a c g a a g a a 407 | | | | | | | | | | | | | | | | | | | | ath-miR5658 1 a u g a u g a u g a u g a u g a u g a a 20	Exon 1
ath-miR5658	3.5		bzip60 386 u c a u g a u g a u g a u g a c g a a 404 | | | | | | | | | | | | | | | | | ath-miR5658 2 u g a u g a u g a u g a u g a u g a a 20	
ath-miR414	7.5		bzip60 389 u g a u g a u g a u g a c g a a g a a g 408 | | | | | | | | | | | | | | | | | ath-miR414 21 u g a c g a u g a u g a u g a a g a u g 2	Exon 1
ath-miR397b	9.0		bzip60 562 u u g a g u g c u u c g u u g c u g 579 | | | | | | | | | | | | | | | | | | ath-miR397b 4 u u g a g u g c a u c g u u g a u g 21	Exon 2

Differential expression levels of predicted miRNAs in response to biotic stress:

To complement our knowledge on miRBase predictions, we quantified the expression levels of predicted miRNAs. We exposed the wild-type Col-0 with pathogen *Pst* DC3000 avrRPM1 up to 6 hours and quantified the expression of miRNAs using stem-loop qRT-PCR technique. The analysis revealed that all three of them are detectable at Arabidopsis leaves without any stress. After six hours the expression levels of all three miRNAs increased highly significantly ($p < 0.0001$). miR414 has the lowest induced expression, while miR5658 has the highest induced expression (figure 1a). While

compared to miR414 and miR397b. The results also demonstrate that miR5658 predominates at transcript accumulation, hence dominates during targeting the *bZIP60*, as miR5658 and miR414 has very overlapping target location (Supplemental figure 1). We opted miR5658 for this investigation because we intended to discover the most crucial regulator of cell death during biotic stress.

The expression of endogenous miR5658 increases concurrently with the duration of biotic stress-triggered cell death:

To strengthen our prediction and better characterize the novel miR5658, we sought a deeper understanding of the accumulation rate of transcripts over time. We collected samples at 0 hours, 2 hours, 4 hours, and 6 hours after exposing wild-type Col-0 to *Pst* DC3000 avrRPM1. For the assessment, a specialized TaqMan assay was utilized. This TaqMan assay is highly specific for mature miR5658, excluding the possibility of having a false-positive assessment of the precursor. In this assay, a stem-loop primer specific to miR5658 was used during reverse transcription. Figure 1b demonstrates that the accumulation of miR5658 transcripts was triggered at two hours and substantially increased in comparison to our control group at six hours. As these results corroborate our initial hypothesis, we intend to continue examining the correlation between miR5658 and *bZIP60* expression.
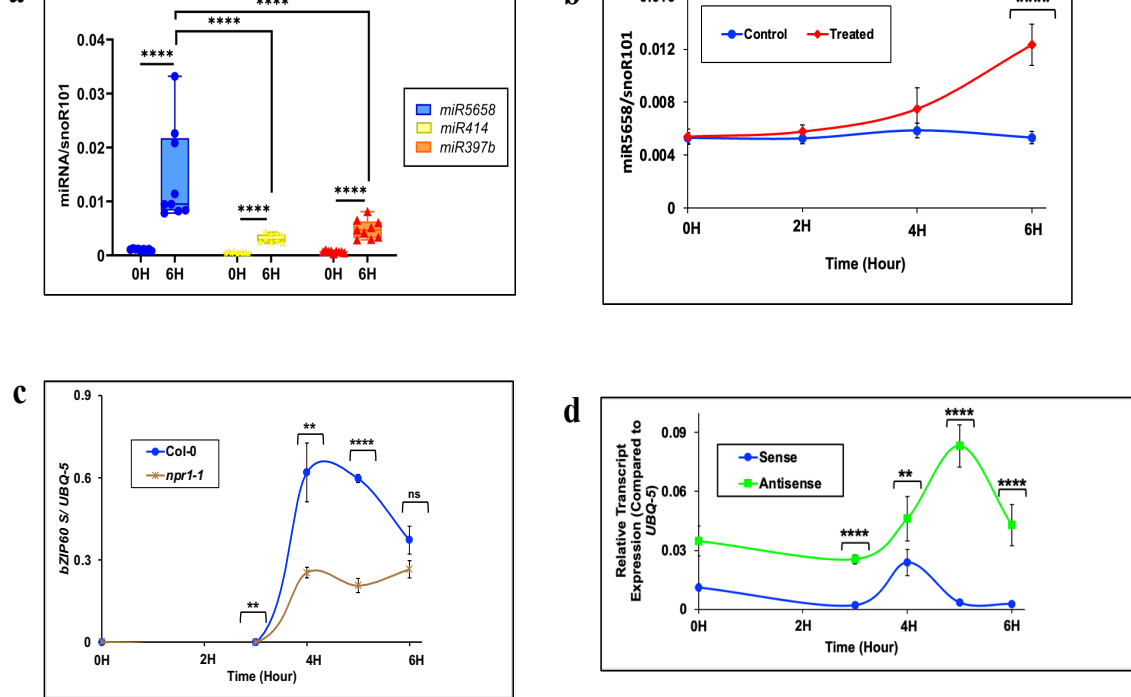
Figure 1: The analysis of relative miRNA expression level. (A) Basal and induced expression of miR5658, miR414, miR397b upon exposure to *Pst* DC3000 avrRPM1 for 0 and 6 hours. Expression levels were measured via stem-loop qRT-PCR and transcript levels were normalized to reference small RNA, snoR101 (a small nucleo-lar RNA). Statistical analyses were performed in GraphPad Prism 9 by Two-Way ANOVA followed by Tukey's multiple comparison test. (B) The expression of miR5658 in a detailed time course upon exposure to *Pst* DC3000 avrRPM1 for 0, 2, 4 and 6 hours. Expression levels were measured via miR5658 specific TaqMan qPCR assay and transcript levels were normalized to reference small RNA, snoR101. Statistical analyses were performed in GraphPad Prism9 by Two-Way ANOVA fol-lowed by Tukey's multiple comparison test. (C) Basal and induced expression of bZIP60 in Col-0 and *npr1-1* genotype upon exposure to *Pst* DC3000 avrRPM1 for 0, 3, 4, 5 and 6 hours. Expression levels were measured via real-time RT-qPCR assay and transcript levels were normalized to reference gene (Ubiquitin-5). Statistical analyses were performed in Excel by two-tailed student t-test. (D) Basal and induced expression of sense and antisense transcript upon exposure to *Pst* DC3000 avrRPM1 for 0, 3, 4, 5 and 6 hours. Expression levels were measured via strand specific real-time RT-qPCR assay and transcript levels were normalized to reference gene (Ubiq-uitin-5). Statistical analyses were performed in GraphPad Prism9 by Multiple Mann-Whitney test. At least three biological replicates with three technical replicates were performed. Significant differences are indicated by asterisks (**** p<0.0001, ***

during cell death triggering stimuli:

bZIP60 transcript has 2 exons and one intron (supplemental figure 2 and 3). After unconventional spicing of *bZIP60* by IRE1 at exon 2, *bZIP60* gets activated as transcription factor. As our predicted miRNAs also target different locations of *bZIP60*, we investigated if the IRE1 splicing location and miRNA target locations are overlapping. miR5658 and miR414 target at exon 1 of *bZIP60* (supplemental figure 1), so these two are excluded from the investigation. Even though miR397b target at exon 2, it does not overlap with the IRE1 splicing site (supplemental figure 1), hence targeting of our predicted miRNA's is independent of IRE1's splicing. Both spliced and unspliced *bZIP60* are vulnerable to degradation/repression by all three miRNAs. To better understand the relationship between miR5658 and spliced *bZIP60* expression, we subjected our positive control wild type Col-0 and negative control immune-compromised *npr1-1* to pathogen *Pst* DC3000 avrRPM1 from zero to six hour to assess the expression through qRT-PCR. The data demonstrate that, the expression of spliced *bZIP60* in genotype Col-0 started to induce highly at three hours, peaks at four hour, gets lower at five and six hours (figure 1c). In mutant *npr1-1* the expression induces higher at four hours and remains almost similar at five and six hours. Spliced *bZIP60* in Col-0 is statistically significantly higher at three, four and five hours than in *npr1-1*. The increased expression of miR5658 (figure 1b) coincide with the decreased expression of *bZIP60* (figure 1c) in wild type Col-0. With this we can hypothesize that miR5658 is the key regulator and act as molecular switch from cell survival to cell death during acute biotic stress.

triggering stimuli:

Then we move forward to characterize the miR5658 and identified a lncNAT serve as a precursor of miR5658, after analyzing the transcripts reported in TAIR 11 database (https://www.arabidopsis.org/index.jsp). The antisense lncNAT (AT4G39838: 2077 bp) is ~95% overlapping with the sense transcript (AT4G39840: 1097 bp) (supplemental figure 4). The miR5658 precursor region in lncNAT is overlapped at the exon of sense transcript. To compare the transcript accumulation of lncNAT and sense transcripts, we exposed wild-type Col-0 plants to the pathogen *Pst* DC3000 avrRPM1 for up to 6 hours and quantified their expression using strand-specific tag-based qRT-PCR (figure 1d). The data suggest that both the lncNAT and sense transcript were expressed at all the time points (0H, 3H, 4H, 5H and 6H) we analyzed them. The lncNAT expresses significantly highly at 3, 4, 5 and 6 hours, compared to sense strand. At 4 hours, the sense transcript expression was relatively elevated, whereas at all other times it was extremely low and flat. At five hours, the lncNAT transcript expression was highest compared to other four timepoints.

Characteristics of sense and antisense mutant lines:

As sense transcript (AT4G39840) is predicted to encode a protein and antisense transcript (AT4G39838) is predicted to transcribe the miiR5658, we generated *srcl* (stress response component-like protein, AT4G39840), which contains T-DNA insertion in the exon and should abolish the expression of sense protein and antisense transcript production (figure 2a). We also generated NAT_{SRCL} (natural antisense transcript of stress

in the precursor region of miR5658 and predicted to exterminate the antisense transcript production (figure 2a). We tested the mutant lines transcript production through quantification of transcripts by using tag-based qRT-PCR before and after cell death inducing abiotic stressor *Pst* DC3000 avrRPM1 up to 6 hours. Figure 2b demonstrate that the expression of miR5658 precursor producing antisense strand is statistically significantly higher after six hours in our positive control wild type Col-0 while treated with *Pst* DC3000 avrRPM1. While the mutant lines *srcl* and NAT_{SRCL} do not show any significant changes in antisense transcript production even after exposure to cell death triggering agent *Pst* DC3000 avrRPM1 (figure 2b). Our negative control *npr1-1* also showed unchanged transcript production upon biotic stressor exposure.

Mutant lines srcl and NAT_{SRCL} is extremely sensitive to prolonged ER stress:

After confirming the mutant lines, we asked whether they exhibit altered ER stress responses. Quantification of total fresh weight and chlorosis followed by chemically induced ER stress are two well established hallmarks of UPR in Arabidopsis [93]. We exposed our positive control wild type Col-0, mutant line NAT_{SRCL}, *srcl* and our negative control mutants *npr1-1*, *bzip60* (figure 2c, 2d and 2e to ER stress caused by chemical tunicamycin (Tm: an inhibitor of N-linked glycosylation, causes ER stress by impeding the folding of glycosylated proteins). First, we wanted to investigate if their total growth rate is impacted by prolonged Tm exposure. We exposed the seedlings to Tm supplemented ½
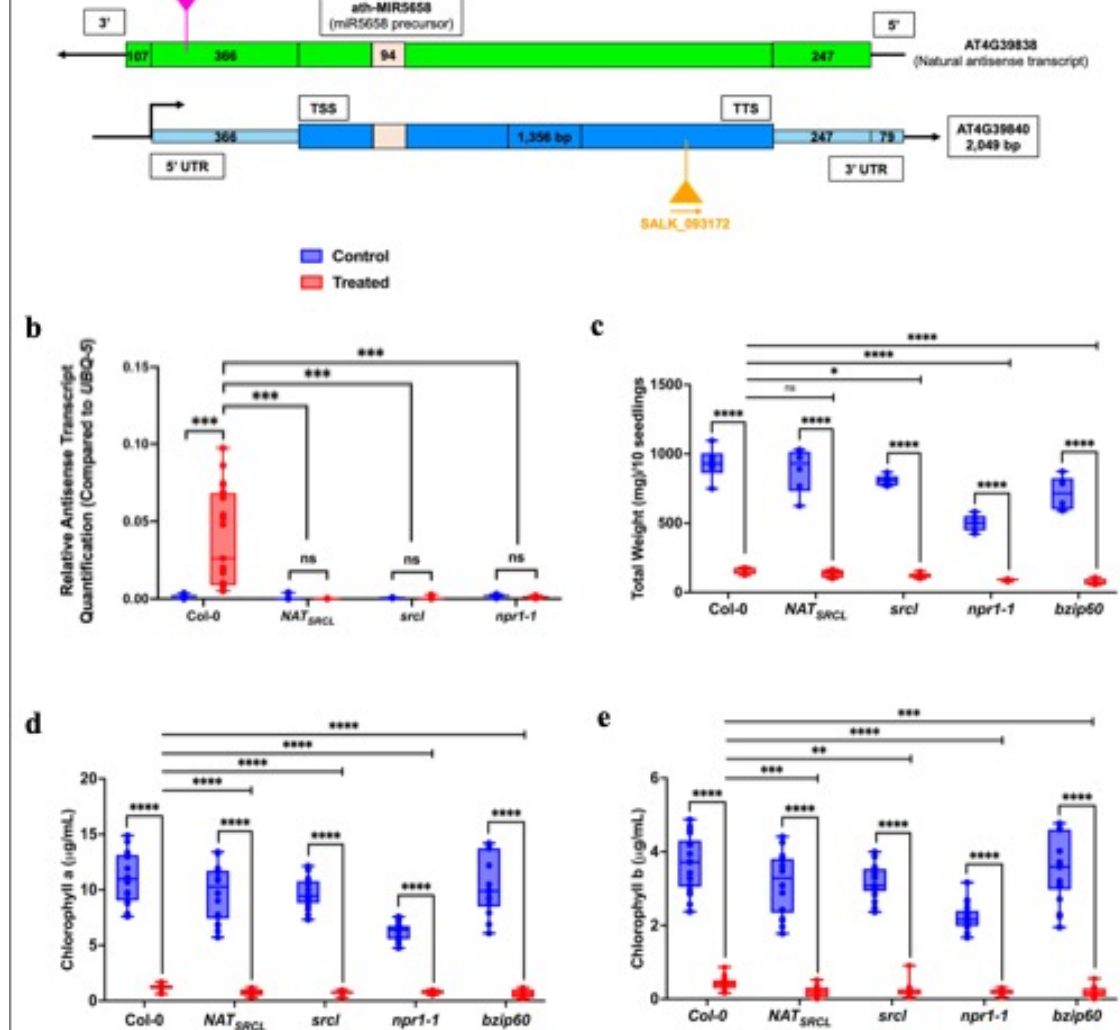
Figure 2: Characterization of *NAT_SRCl* and *srcl* mutants: (A) Schematic of miR5658 precursor NAT (antisense) and its sense transcript with the T-DNA insertion location. (B) Total weight (mg/10 seedlings) of different 5 days old plants upon exposure to Tunicamycin for 3 days and recovery of 3 days. Statistical analyses were performed in GraphPad Prism9 by multiple Mann-Whitney test. (C) and (D) Chlorophyll a (µg/ml) and chlorophyll b (µg/ml) of different 5 days old plants upon exposure to Tunicamycin for 3 days and recovery of 3 days. Statistical analyses were performed in GraphPad Prism9 by multiple Mann-Whitney test.

MS

strate that all the mutants along with our positive control wild type Col-0 are severely affected, and the total weights reduced statistically significantly by Tm induced ER stress.

with Tm stressed wild type Col-0 to Tm stressed NAT_{SRCL} they impact is not statistically significant. Possibly due to prolonged ER stress the miR5658 in Col-0 unable to substantiate the humongous amount of ER stress. On the contrary the total weight of sense mutant line *srcl* is statistically significantly impacted compared to Tm stressed Col-0, which indicates that the sense transcript is associated with prolonged ER stress management. Our other two negative control mutants *npr1-1*, *bzip60* were severely statistically significantly affected by Tm stress compared to Col-0. The mutant lines are deficient in ER stress recovery compared to our positive control wild type Col-0.

Next, we investigated the amount of seedling chlorosis because of Tm mediated ER stress by quantifying chlorophyll a and chlorophyll b content. Chlorophyll a content in mutant line NAT_{SRCL} and *srcl* reduced statistically significantly compared to wild type Col-0 (figure 2d). Negative control mutants *npr1-1* and *bzip60* also showed significant chlorosis compared to Col-0, even compared to NAT_{SRCL} and *srcl* (figure 2d). The mutant line NAT_{SRCL} and *srcl* showed significant chlorosis in terms of Chlorophyll b when compared to Col-0 (figure 2e). Negative control mutants *npr1-1* and *bzip60* again showed significant chlorophyll b reduction compared to Col-0 (figure 2e). But chlorosis of chlorophyll a was higher in all mutant lines compared to wild type (figure 2d and 2e).

Mutation in the miR5658 targeted seed region in bZIP60 blocks the miR5658 targeting and increase bZIP60 expression:

Afterwards, we seek to comprehend the causal relationship between miR5658 and the *bZIP60* transcript. To understand the miR5658's ability to degrade *bZIP60* during cell

the hypothesis that the mutated *bZIP60* will be able to escape the miR5658 degradation. The seed region of miR5658 is comprised of a total of four aspartic acids, making it a one-of-a-kind binding site. Which makes it hard to make any synonymous point mutation that will block miR5658 binding to *bZIP60*. To verify that miR5658 is being blocked, we used a combination of two-point mutations and two sets of mutated *bZIP60* (M1 and M2). We used site directed mutagenesis to mutate wilt type *bZIP60* into M1 and M2. The mutations in the pDNOR207 constructs were validated by sanger sequencing. Next, we generated GUS constructs carrying 35S promoter followed by WT/M1/M2 *bZIP60* transcript fused with GUS (2X35S::WT *bZIP60*-GUS; 2X35S::M1 *bZIP60*-GUS; 2X35S::M2 *bZIP60*-GUS) (supplemental figure 5), incorporated them into *Agrobacterium tumefaciens* and infiltrated them into different genotypes of 4-5 weeks old Arabidopsis and the GUS expression pattern was evaluated. The transient MUG assay result demonstrates that wild type Col-0, sense mutant *srcl*, negative control mutant *bzip60* showed significantly higher mutated *bZIP60* expression compared to wild type *bZIP60*, whereas our miR5658 mutant line NAT_{SRCL} has significantly lower expression of mutated *bZIP60* than wild type *bZIP60* (figure 3a). Another control mutant *npr1-1* showed unchanged expression of *bZIP60*, which demonstrated extremely higher *bZIP60* expression (both in wild type and mutated) compared to any other genotypes (figure 3b).

We investigated the reason behind the reduced expression of mutated M2 *bZIP60* in NAT_{SRCL}, miR5658 and miR414 has overlapping seed region (updated supplemental 1). miR414 possibly compete with miR5658 for binding to the seed region of *bZIP60*. As miR414 has significantly lower transcript accumulation than miR5658, it cannot perform

cilitates miR414 to bind and perform to its full potential. We confirmed their binding
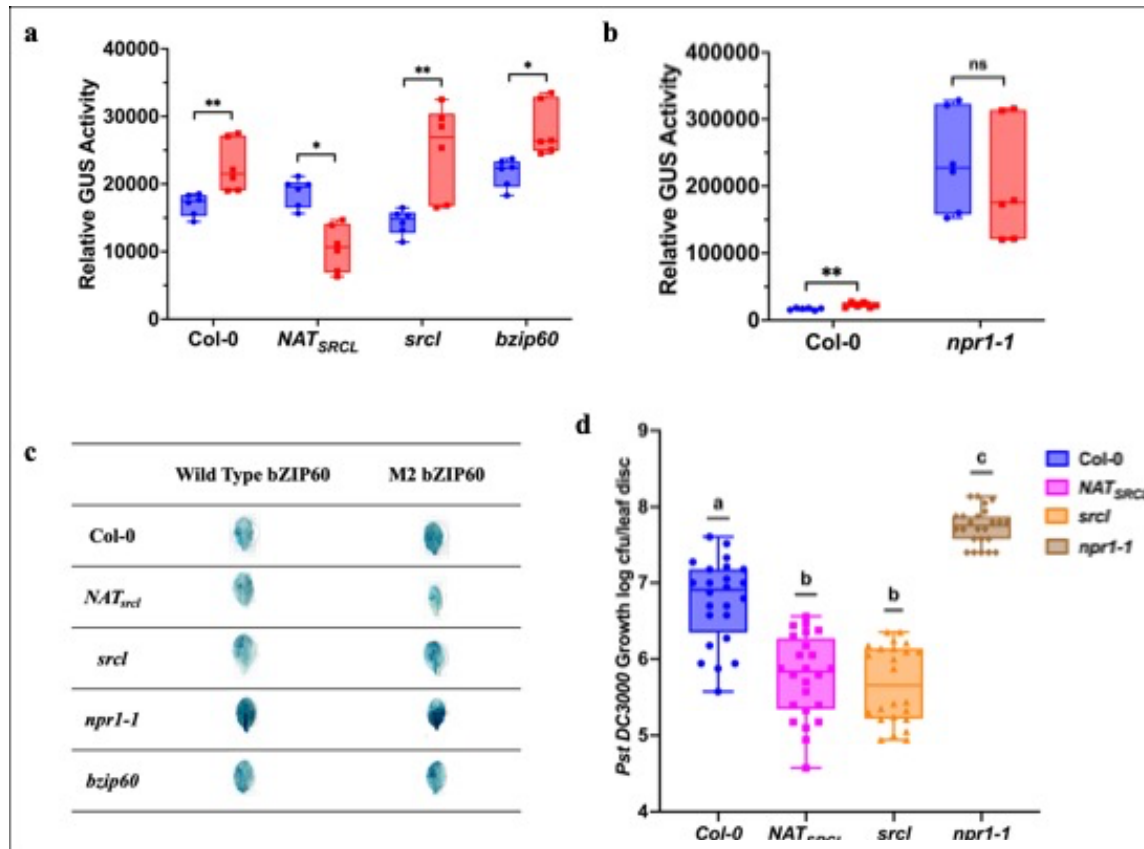

Figure 3: Transient activity of mutated bZIP60 and pathogenic resistance: (A) and (B) Transient MUG assay to determine the wild type and mutant bZIP60 expression in presence/absence of miR5658. Quantification of ß-glucuronidase (GUS) activity in Arabidopsis Col-0, NAT_{SRCL}, srcl, npr1-1 and bZIP60 leaves transiently expressing transcriptional 35S::WT bZIP60-GUS and 35S::M2 bZIP60-GUS reporter. Statistical analyses were performed in Excel by two-tailed student t-test. (C) Histochemical GUS assay in Col-0, NAT_{SRCL}, srcl, npr1-1 and bZIP60 leaves transiently expressing transcriptional 35S::WT bZIP60-GUS and 35S::M2 bZIP60-GUS reporter. (D) Enhanced disease resistance of different genotypes upon exposure to Pst DC3000. Bacterial populations were quantified at 2 dpi. Statistical analyses were performed in Excel by One-Way ANOVA followed by Tukey's multiple comparison test. Treatment groups are represented according to legends. 4-5 weeks old plants were used to perform the experiment. At least three biological replicates with three technical replicates were performed. Significant differences are indicated by asterisks (**** $p<0.0001$, *** $p<0.001$, ** $p<0.01$, * $p<0.05$) or by letters (a/b/c) for dif-

bZIP60.

To supplement the transient MUG assay results we performed histochemical GUS assay with the genotypes Col-0, NAT_{SRCL}, *srcl*, *bzip60* and *npr1-1* harboring WT *bZIP60* (2X35S::WT *bZIP60*-GUS), M1 *bZIP60* (2X35S::M1 *bZIP60*-GUS) and M2 *bZIP60* (2X35S::M2 *bZIP60*-GUS) respectively. Figure 3c demonstrate that, the Col-0 harboring M2 *bZIP60*: GUS showed a remarkable increase in GUS expression with compared to WT *bZIP60*. The NAT_{SRCL} harboring WT *bZIP60* showed higher *bZIP60* expression compared to M2 *bZIP60*, which complements MUG assay data. The sense mutant line *srcl* harboring M2 *bZIP60* has significantly higher expression of *bZIP60* compared to WT *bZIP60*. Another control mutant *bzip60* harboring M2 *bZIP60* showed comparatively higher GUS levels than WT *bZIP60*. While our negative control mutant *npr1-1* showed unchanged GUS expression harboring WT *bZIP60* and M2 *bZIP60*. All the data supplemented above narrow down to the conclusion that miR5658 can directly bind to WT bZIP60 and block the bZIP60 translation or degrade it.

Antisense and sense mutant lines are more resistant towards biotic stress inducing pathogen Pseudomonas syringae:

We next aimed to study the involvement of miR5658 and its sense transcript in pathogen resistance mechanisms. We pressure infiltrated *Pst* DC3000 into the leaves of our wild type positive control Col-0, mutant lines NAT_{SRCL}, *srcl* and hypersusceptible *npr1-1* followed by bacterial growth quantification after three days of infiltration [94]. Our miR5658 mutant line NAT_{SRCL} demonstrates more than half log lower bacterial growth

mutant line *srcl* showed about one log lower bacterial growth compared to Col-0. With lower bacterial loads the mutant lines showed higher resistance against pathogen infection compared to Col-0. In these mutants as the miR5658 and/or its sense transcript is absent, their pro-survival pathway is active longer than the positive control. The pro-survival pathways help the plants to resist more than the control Col-0. Our negative control *npr1-1* showed highest amount of bacterial growth as it was expected to be the most susceptible genotype.

miR5658 and its sense transcript regulate HR mediated cell death:

After having the direct evidence that miR5658 can bind to *bZIP60*, next we seek to comprehend the pivotal regulatory role of miR5658 in the progression of cell death. To investigate the function of miR5658 in HR mediated cell death we challenged our miR5658 mutant line NAT_{SRCL}, sense mutant line *srcl*, Col-0 and *npr1-1* to the pathogen *Pseudomonas syringae* pv. tomato (*Pst*) DC3000 harboring the effector AvrRpm1. The levels of cell death upon pathogen infection were quantified by electrolyte leakage measurement. As the dying cells release electrolyte, the amount of leaked electrolyte is directly comparable to the amount of dying cells. The mutant NAT_{SRCL} suppressed the extent of cell death caused by the avirulent pathogen *Pst* DC3000 avrRPM1 (figure 4a). The sense mutant *srcl* also suppressed the cell death progression compared to our positive control Col-0 and negative control *npr1-1*. Both NAT_{SRCL} and *srcl* mutant showed delayed cell death started to noticeable as early as four hours post inoculation compared to our control genotypes. Our wild type Col-0 showed steep progression toward cell death at

avrRPM1 exposure. In case of *npr1-1* they arrive at plateau around six hours and 30 minutes. *npr1-1* showed higher cell death progression and wild type Col-0 has comparable progression to *npr1-1*, while the *NAT*$_{SRCL}$ showed lowest progression and *srcl* has comparable progression with *NAT*$_{SRCL}$. As in the mutant lines are deficient in miR5658 production, their *IRE1/bZIP60* mediated survival pathway in still active which delayed
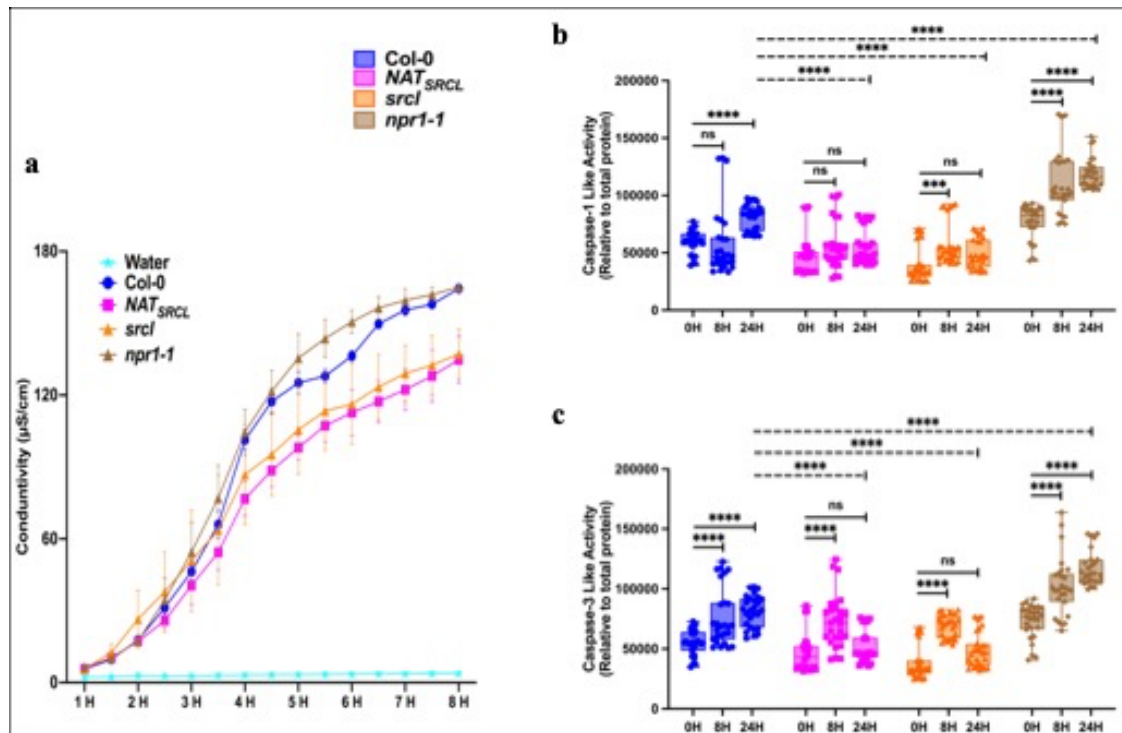

Figure 4: Cell Death Analysis of control and mutant lines. (A) Electrolyte leakage from Col-0, *NAT*$_{SRCL}$, *srcl* and *npr1-1* after bacterial inoculation. 4-5 weeks old Arabidopsis leaves were syringe-infiltrated with *Pst* DC3000 avrRPM1. Conductivity measurements of electrolytes leakage from dying cell were recorded from 1 to 8 hour after inoculation. (B) and (C) The levels of Caspase-1 and Caspase-3-like activity in the total protein content at 0, 8 and 24 hours were measured in Col-0 *NAT*$_{SRCL}$, *srcl* and *npr1-1* Arabidopsis plants following bacterial inoculation. Syringe infiltration of *Pst* DC3000 avrRPM1 was performed on 4-5-week-old Arabidopsis leaves. Statistical analyses were performed in GraphPad Prism9 by multiple Mann-Whitney test. At least three biological replicates with three technical replicates were performed. Significant differences are indicated by asterisks (**** $p<0.0001$, ***

sense transcript plays significant role in regulating HR mediated cell death.

There is evidence that in HR mediated cell death during ER stress caspase-like activities are involved in plants. So, to substantiate the electrolyte leakage data, next we aimed to quantitate protease activity in dying cells [95-97]. To do that, we exposed our wildtype control Col-0, miR5658 mutant line NAT_{SRCL}, sense mutant line *srcl* and hypersensitive mutant *npr1-1* to the pathogen *Pst* DC3000 harboring the effector AvrRpm1 for eight hours and 24 hours. As in Arabidopsis caspases are not identified, we used synthetic tetrapeptide sequence (DEVD), based on caspase-1 and caspase-3 cleavage site for the quantification of caspase-1/caspase-3 like protease activity in Arabidopsis. In wild type Col-0 caspase-1 like activity remain unchanged at eight hours, while gets highly statistically significantly induced at 24 hours (figure 4b). miR5658 mutant line NAT_{SRCL} showed unchanged caspase-1 like activity for both eight and 24 hours. Sense mutant line *srcl* showed increased caspase-1 like activity at eight hours, but unchanged activity at 24 hours. Our hypersensitive control mutant *npr1-1* has increased caspase-1 like activity at both eight and 24 hours. The wild type Col-0 showed significantly higher caspase-1 like activity at 24 hour compared to NAT_{SRCL}, *srcl*; while Col-0 has lower caspase-1 like activity compared to control mutant *npr1-1*.

In case of caspase-3 like activity, the wild type Col-0 caspase-3 like activity gets highly induced both at eight hours and at 24 hours (figure 4c). miR5658 mutant line NAT_{SRCL} showed induced caspase-3 like activity at eight hours, which goes down at 24 hours. Sense mutant line *srcl* showed increased caspase-3 like activity at eight hours, but unchanged at 24 hours. Our hypersensitive control mutant *npr1-1* has increased caspase-1

Should we remove caspase-3 graph?

Because the NAT_{SRCL} line does not have miR5658 their protease like activity is absent, while in the sense mutant line *srcl* their protease like activity is reduced/absent. The sense mutant line *srcl* showed comparable caspase-1/caspase-3 like activity with NAT_{SRCL}, possibly because of the sense transcripts cognate mode of expression. Which further concludes to their slower cell death progression during HR induced cell death.

Differential expression of IRE1a, bZIP60 and cell death markers upon cell death induction:

Then we set out to investigate the differential expression level of *IRE1a* as response to cell death triggering stimuli by challenging the different genotypes (wild type Col-0, miR5658 mutant line NAT_{SRCL}, sense mutant line *srcl*, hypersensitive mutant *npr1-1* and *bzip60*) with *Pst* DC3000 AvrRpm1. We collected the samples at zero, three, four, five and six hours and quantified *IRE1a* expression levels through qRT-PCR. At three hours the *IRE1a* in NAT_{SRCL} is induced statistically significantly higher compared to wild type Col-0 and the induction level gets higher at six hours (figure 5a). Which indicates that due to miR5658 absence in NAT_{SRCL} their induced *IRE1a* is activating the pro-survival pathway as well as resisting cell death. The sense transcript mutant *srcl* induced similar level of *IRE1a* while compared with Col-0 at three hours, but at six hours they induced statistically significantly higher amount of *IRE1a*. At six hours the NAT_{SRCL} and
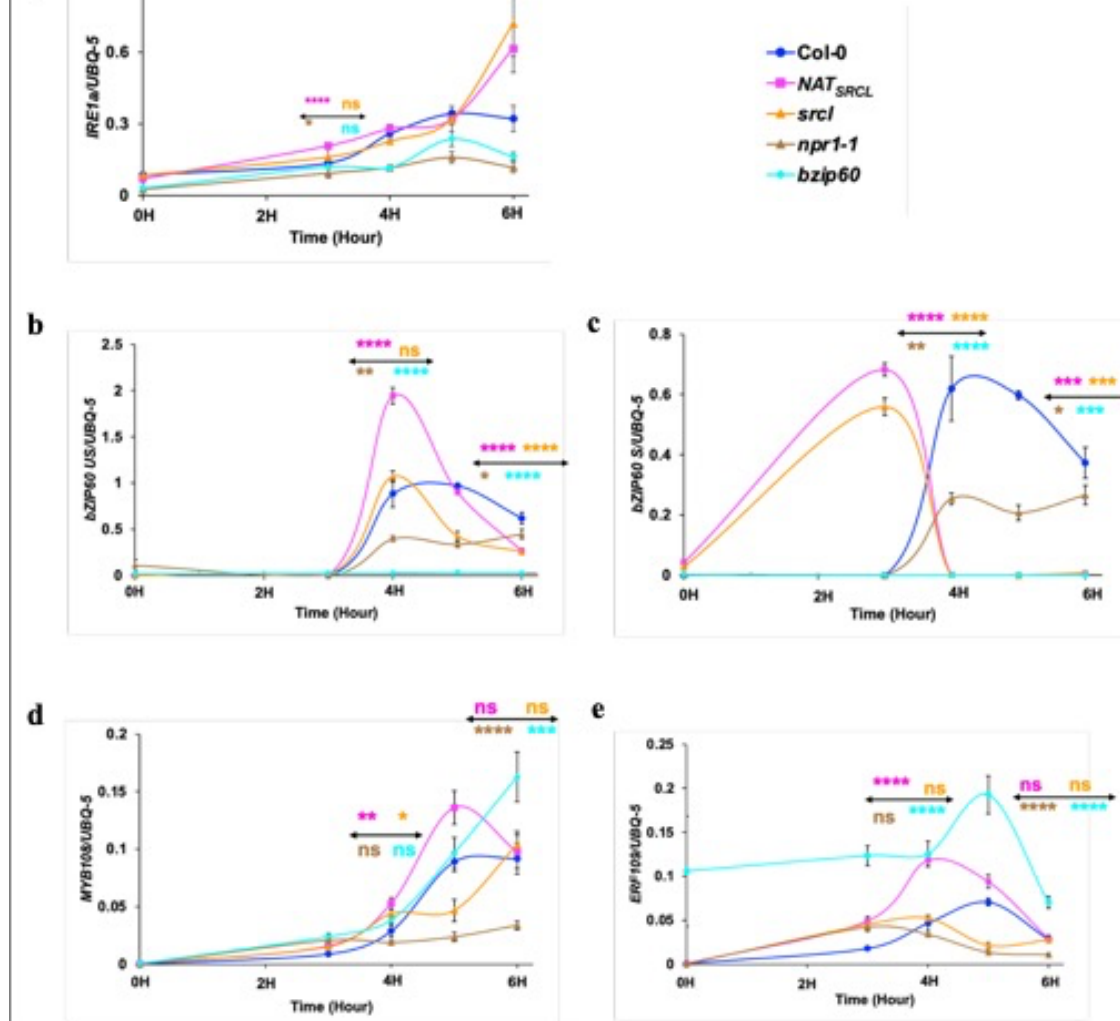
Figure 5: Upstream and downstream signaling markers quantification: The expression quantification of (A) IRE1a, (B) bZIP60 unspliced, (C) bZIP60 Spliced, (D) MYB108 and (E) ERF109 in Col-0, NAT_{SRCL}, srcl, npr1-1 and bZIP60 leaves upon exposure to *Pst* DC3000 avrRPM1 for 0, 3, 4, 5 and 6 hours. Expression levels were measured via qRT-PCR and transcript levels were normalized to reference gene (Ubiquitin-5). Statistical analyses were performed in Excel by two tailed student t-tests. Treatment groups are represented according to legends. 4-5 weeks old plants were used to perform the experiment. At least three biological replicates with three technical replicates were performed. Significant differences are indicated by asterisks (**** $p<0.0001$, *** $p<0.001$, ** $p<0.01$, * $p<0.05$).

srcl produced similar level of *IRE1a*, which refers to their concordant kind of function.

The hypersensitive mutant npr1-1 showed statistically significantly reduced level of

IRE1a expression throughout the timepoints.

Then we quantified the expression level of *bZIP60*, another crucial gene in po-survival pathway. As *bZIP60* go through an unconventional splicing by *IRE1*, we quantified both unspliced (US) and spliced (S) *bZIP60* upon cell death triggering stimuli. The *NAT*$_{SRCL}$ induced statistically significantly higher amount of unspliced *bZIP60* at four hours, but at six hours they had statistically significantly lower amount compared to wild type Col-0 (figure 5b). While *NAT*$_{SRCL}$ showed highest amount of spliced *bZIP60* at three hours, which goes down at four and subsequent hours (figure 5c). As *NAT*$_{SRCL}$ showed highest amount *IRE1a* at three hours (figure 5a), which explains the highest amount of spliced *bZIP60* at three hours, highly expressed *IRE1a* spliced higher *bZIP60* to activate and sustain the pro-survival pathway. The mutant line *srcl* showed higher amount of unspliced *bZIP60* at four hours (figure 5b), while at three hours they had higher amount of spliced *bZIP60* (figure 5c), compared to wild type Col-0. They also expressed higher amount of *IRE1a* at three hours (figure 5a). Even though the mutant line *srcl* showed higher amount of *IRE1a* and subsequent spliced *bZIP60*, the expression was lower than *NAT*$_{SRCL}$, which refers that the antisense transcript supports the function of miR5658. The hypersensitive mutant *npr1-1* showed lower level of both unspliced and spliced *bZIP60* (figure 5b and 5c) along with *IRE1a* (figure 5a). Another control mutant *bzip60* showed minimal or zero expression throughout the time (figure 5b and 5c).

After correlating the expression of *IRE1a* and *bZIP60*, we aimed to quantify two cell death triggering markers MYB domain protein 108 *(MYB108)* and ethylene response

known as a negative regulator of cell death [98-100]. At four hours the expression of *MYB108* is statistically significantly higher in NAT_{SRCL} than wild type Col-0, which goes up at five hours but goes down close to Col-0 at six hours (figure 5d). Which refers that the NAT_{SRCL} is triggering cell death stress signaling earlier and stronger than Col-0, to activate/sustain the pro-survival pathway and slower the cell death rate. While the sense mutant *srcl* showed higher amount of *MYB108* at four hours, stays stable till five hours and goes up at six hours; but stays closer to Col-0 and NAT_{SRCL} at six hours (figure 5d). The *npr1-1* mutant showed lowest expression of *MYB108* throughout the timepoints (figure 5d). Another control mutant *bzip60* showed highest expression of *MYB108* at six hours which started to consistently increase from three hours.

ERF109 delays PCD by regulating of PCD-inhibitor gene and help plants to adapt to salt stress [101,102]. So sought to quantify the expression of *ERF109* in our experiments. NAT_{SRCL} showed statistically significantly higher expression of *ERF109* at four hours and goes down at five and six hours closer to wild type Col-0 (figure 5e). The sense mutant *srcl* had *ERF109* expression closer to Col-0 at four hours and then goes down at five hours and remains same at six hours. Hypersensitive mutant *npr1-1* showed lower level of *ERF109* throughout the timepoints, while mutant *bzip60* showed highest expression of *ERF109* throughout the timepoints. The higher amount of *ERF109* in NAT_{SRCL} delayed the cell death in miR5658 deficient line as well as sustaining the pro-survival pathway, while mutant *bzip60* would require more *ERF109* to delay the cell death due to absence of *bzip60*.

Eukaryotic cells must maintain cellular homeostasis during developmental and stress condition, specifically maintaining ER homeostasis is very critical for plants growth, development, and survival. Within the three distinct pathways, IRE1 is the oldest and most conserved branch of UPR in eukaryotes that maintains ER homeostasis [103]. Numerous investigations in mammalian system have demonstrated that ER stress is shaped by miRNA-mediated regulations, and that ER stress additionally governs the expression of miRNAs [104]. Several miRNAs (miR-214, miR-30-c-2*, miR-34c-5p, miR-665, miR-1291) has been discovered to be directly involved with the regulation of IRE1 and XBP1 [88-92]. But in Arabidopsis there is there is no detailed study highlighting the regulatory roles of miRNA during ER stress response. lncRNAs are very widespread both in prokaryotic and eukaryotic organisms in terms of their functions and key regulatory roles. However, the functions of ER stress response lncRNAs in Arabidopsis have not been extensively investigated to date. The present study aims to investigate the role of a specific miRNA (miR5658) derived from a novel lncNAT in shifting the response of the IRE1/*bZIP60* pathway from pro-survival to pro-death during acute endoplasmic reticulum (ER) stress induced by a biotic stressor in Arabidopsis.

Through bioinformatics analysis we investigated the potential miRNAs that can target *bZIP60* as well as regulate IRE1/*bZIP60* mediated pro-survival pathway. We identified three different miRNAs (miR5658, miR414, miR397b) that can target *bZIP60* transcript (Table 1). All three of them originate from three different lncRNA. miR414 family is highly conserved across plant system, has five homologs, two of them are from

ported to negatively regulate the heat shock protein 90.1 (AtHSP90.1) at the early proteo-toxic stress condition [106]. miR397 family is highly conserved and has two members miR397a and miR397b (both of them are localized in chromosome IV), there is only one nucleotide difference in-between miR397a and miR397b [107]. miR397b is reported to regulate flowering in Arabidopsis and is anticipated to play crucial roles in enhancing the overall fitness of plants [108], while OsmiR397 have been reported to be involved with the regulation of seed size, grain yield and early flowering in rice [109,110]. miR5658 has been found on *A. thaliana*, *Brassica rapa*, eggplant and *Cannabis sativa. L* [111-115]. In *Cannabis sativa. L* five members of miR5658 has been identified and predicted to target important transcription factor (TF) groups (MYB and GRAS family), BAK1-interacting receptor like kinase 1, serine/threonine protein phosphatase, dof zinc finger protein, nucleotide-binding site-leucine-rich repeat (NBS-LRR) domain [114]. All these targets are associated with plant development, metabolism, hormonal signaling, membrane receptors and channels regulation, transcriptional regulation, hypersensitive response and apoptosis [114]. miR5658 has been documented to directly stimulate the expression of the AT3G25290 gene by specifically targeting its promoter region [115]. In eggplant miR5658 has been reported for their negative roles to the host immunity suppression infected by wilt-causing pathogen *Ralstonia solanacearum* [112]. While miR5658 has not been studied in detail yet, it originates from a NAT (lncNAT) a type of lncRNA. After analyzing the differential expression level of miR5658, miR414 and miR397b, we focused on miR5658 as it showed exceptionally highest level of induced expression. Moreover, it has already been predicted for the involvement of hypersensitive response, apoptosis and showed contribution

the expression of lncNAT transcript, miR5658 and *bZIP60* (figure 1b, 1c and 1d), we concluded that the mir5658 and *bZIP60* showed a reciprocal relationship, which supported our hypothesis primarily.

Among very wide range of functions, regulating the expression of target gene is one of the most identified functions of lncNAT [116,117]. To provide more evidence to support our hypothesis we next analyzed the function of miR5658 in (T-DNA insertion) mutant line NAT_{SRCL}, the sense transcript (T-DNA insertion) mutant line *srcl* during abiotic and biotic stress. The NAT_{SRCL} mutant exhibits insensitivity to prolonged ER stress induced by Tm, whereas the sense transcript *srcl* displays sensitivity to prolonged Tm-mediated ER stress (figure 2c, 2d and 2e).

To further substantiate the existing evidence, our transient MUG and GUS assay results demonstrated that the mutation in *bZIP60* hinders the binding and functional activity of miR5658 (figure 3a, 3c). Surprisingly, the transient expression of *bZIP60* in the miR5658 mutant NAT_{SRCL} is lower than expected, possibly indicating a binding competition between miR5658 and miR414 (figure 3a). Due to the nearly complementary binding site of miR5658 and miR414, and the higher expression level of miR5658 compared to miR414, when the seed region of miR5658 is mutated and its binding is blocked, miR414 seizes this opportunity to bind to the mutated *bZIP60*, resulting this reduced expression (supplemental figure 6 and 7). In the context of pathogen resistance, the mutant lines NAT_{SRCL} and *srcl* demonstrated enhanced resistance, indicating their adverse impact on host resistance (3d). A previous investigation conducted on eggplant exhibited a

highlights the involvement of miR5658 in regulating hypersensitive cell death.

Multiple studies have documented the generation of an "oxidative burst" occurring during both the early and late stages of plant-pathogen interactions. Furthermore, these studies have highlighted the involvement of reactive oxygen species (ROS) in the regulation of cell death responses and signaling pathways. Moreover, the disturbance of cytosolic ionic homeostasis is identified as a pivotal event in the process of HR-mediated cell death. [7,118-121]. Our findings revealed a reduction in leaked ions during HR mediated cell death within the mutant lines NAT_{SRCL} and *srcl*, indicating an elevated resistance level in these mutants (figure 4a). Caspases are a class of intracellular proteases that play a crucial role in initiating various signaling cascades involved in programmed cell death, cell proliferation, and inflammation. Despite the absence of established caspases in plant genome sequencing data (Uren et al., 2000), the occurrence of caspase-like proteolytic activity has been observed in plant cell death processes associated with hypersensitive response (HR) and disease [122,123]. Our findings demonstrate that NAT_{SRCl} exhibits minimal to no caspase-1 and caspase-3-like activity at eight and 24 hours. Similarly, *srcl* displays minimal activity at eight hours and no activity at 24 hours, respectively (figure 4b and 4c). These evidence supports the conclusion that miR5658, in conjunction with its sense transcript, promotes the transition from a pro-survival pathway to a pro-death pathway. To investigate the interplay between *IRE1a*, *bZIP60*, miR5658, and downstream signaling genes, we quantified their expression levels over a time course ranging from zero to six hours. In the miR5658 mutant line NAT_{SRCl}, we observed elevated expression of *IRE1a* at three hours, the highest level of *bZIP60* splicing at three hours, and a

(figure 5a, 5b, 5c, 5d and 5e). In the sense transcript mutant srcl, we observed higher expression of *IRE1a* at three hours and increased *bZIP60* splicing at three hours. Additionally, there was an increase in the expression of downstream signaling genes MYB108 and ERF109, although the differences were not statistically significant. Taken together, these data suggest that the absence of miR5658 in the mutant line NAT_{SRCl} results in a prolonged maintenance of the pro-survival pathway compared to the wild-type Col-0.

Furthermore, we assessed the expression of IRE1b to investigate any potential relationship, but we observed consistently low/minimal levels of IRE1b expression across different genotypes from zero to six hours. These findings suggest that there is no direct relationship between IRE1b expression and miR5658 expression. To investigate the possibility of miR5658 targeting the promoter region of *IRE1a*, we conducted prediction analysis using miRBase and psRNATarget website. The analysis revealed that miR5658 has the potential to target the promoter region of *IRE1a*, specifically around 38 base pairs upstream of the transcription start site. Based on a previous study by Yang et al. (2019) demonstrating the regulatory role of miR5658 in gene expression through targeting the promoter region, we propose that miR5658 has the ability to modulate the expression of *IRE1a* in an upregulating or downregulating manner when necessary. Interestingly the bZIP, WRKY family has been identified as a potential cis-regulatory element of miR5658 homologs in Cannabis, as predicted by computational analysis [114]. Therefore, our prediction suggests that members of the bZIP/WRKY family, such as bZIP17 and bZIP28, may play a role in regulating the expression of miR5658 in response to ER stress conditions. Consequently, miR5658 can modulate the transcription factor *bZIP60*,

Additionally, miR5658 may also be involved in regulating the expression of *IRE1a* when necessary.
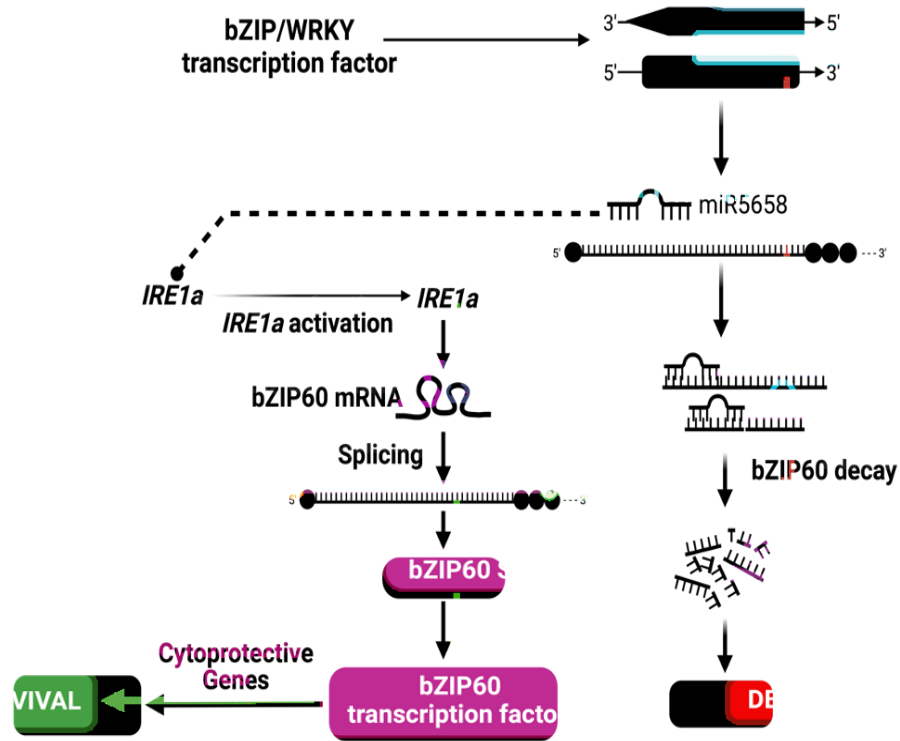

Figure 6: The proposed model for miR5658 expression and activity.

Materials and Methods

Plant Material and Growth Conditions:

In this study, the wild-type accessions of Arabidopsis thaliana (L.), specifically Columbia-0, were utilized. The NAT_{SRCl} and *srcl* T-DNA insertion line with the accession code SALK_047112, SALK_093172 respectively, were obtained from Arabidopsis

Every seed was planted individually in pots containing sterilized soil (SunGro Horticulture, Super-Fine Germinating Mix). The seeds were stratified in a cold room facility at a temperature of 4°C for a duration of seven days. Subsequently, the pots were relocated to a controlled growth room facility with specific conditions including a 12-hour light and 12-hour dark photoperiod, a temperature of 21°C, a light intensity of 100 µmol/m^2/s, and a relative humidity of 40%. Seedlings aged between 10 and 15 days were then transferred into 72-well flats for growth over a period of one month, during which subsequent experimentation took place.

miRNA Expression Analysis:

Stem-loop RT-PCR was employed to analyze the expression of miR5658, miR414, and miR397b. Total RNA extraction was carried out using the previously described method [124]. Following that, the stem-loop RT-PCR analysis protocol was adapted from Chen et al. (2005)[125]. Briefly, leaf tissue was collected from one-month-old plants at specific time points for the designated genotype, treatment, and time point combinations. At least three leaves were obtained from three independent plants for each combination. Total RNA was extracted using Trizol reagent from Invitrogen, and DNase I from Ambion was utilized to eliminate DNA contaminants. For reverse transcription, 3.33 µg of total RNA was utilized and transcribed using the SuperScript III first-strand RT-PCR kit from Invitrogen. Quantitative gene expression analysis was conducted using GoTaq qPCR Master Mix from Promega, along with miRNA-specific primers, in a RealPlex S MasterCycler (Eppendorf). To ensure equal RNA input, snoR101, a small nucleolar

ues were normalized to the expression of snoR101 to account for variations in RNA input. The bZIP60 splicing assays were conducted following the methodology described in Moreno et al.[23]. In summary, a shared forward primer was utilized alongside a set of reverse primers designed to selectively bind to either the unspliced or spliced forms of the cDNA derived from bZIP60 mRNA. This approach facilitated the identification of two distinct qRT-PCR products representing the unspliced and spliced variants of bZIP60 (supplemental figure 3). The primer sequences utilized for qRT-PCR analysis can be found in Supplementary Table 1.

TaqMan Assay for miR5658 Expression Analysis:

The expression of miR5658 was quantified using a specific TaqMan assay designed for miR5658. Total RNA extraction and DNase I treatment were carried out following the aforementioned protocol [124]. The protocol used in this assay was adapted from Fisher Scientific. In brief, the reverse transcription master mix consisted of the following components: 0.15 µL of 100 mM dNTP mix, 4.16 µL of nuclease-free water, 1.00 µL of multiscribe reverse transcriptase, 1.50 µL of 10X reverse transcriptase buffer, 0.19 µL of Rnase inhibitor, and 3 µL of the corresponding RT primer provided. For the RT reaction, 5 µL of RNA was added to 10 µL of the RT master mix. The qPCR master mix was prepared by combining 7.67 µL of nuclease-free water, 1.00 µL of TaqMan microRNA assay (20X), 10.00 µL of TaqMan 2X universal PCR master mix, and 1.33 µL of the RT reaction product. Means and standard errors were calculated based on three replicate measurements per genotype.

Sense and antisense transcript quantification:

To quantify the sense and antisense transcript we used strand specific tag-based RT-PCR. Total RNA extraction and DNase I treatment were performed in accordance with the previously described protocol [124]. The procedure for synthesizing cDNA involves a reaction that includes the following components: 3µM transcript-specific tagged primer, 1 µg RNA, 5X first strand buffer, 0.1M DTT, 10mM dNTP, superscript III reverse transcriptase (200U/l), RNase inhibitor (40U/l) and nuclease-free water. Following the reverse transcription (RT) reaction, exonuclease (20U) was applied to deactivate any unbound reverse transcription primers. The mixture for quantitative PCR (qPCR) includes the products of reverse transcription, both forward and reverse primers, the GoTaq qPCR Master Mix sourced from Promega, and nuclease-free water. The Ct values were adjusted to correspond to the ubiquitin 5 (UBQ5) gene. The primer sequences utilized for qRT-PCR analysis can be found in Supplementary Table 1.

Assays for measuring ER stress Analysis:

Seeds from various Arabidopsis strains underwent a cleansing process using 70% Ethanol and 0.05% Triton. Following this, they were placed on half-strength solid Murashige Skoog (MS) (Phyto- technology Labs, Overland Park, KS, USA) media plates and stratified at a temperature of 4 °C for a period of 3 days. Upon completion of the stratification process, the MS plates were moved to growth chambers for growth for 5 days. These chambers were maintained under specific conditions: a 12-hour light/12-hour dark cycle, a consistent temperature of 21 °C, a light intensity of 100 µmol/m2/s, and a

ployed at a concentration of 0.30 μg/mL as a chemical inducer of ER stress. Five-day-old

seedlings were transitioned to a liquid half-strength MS medium, either with or without

the appropriate concentration of Tm. They were then left to this medium for a duration of

three days. After a three-day period, the seedlings were relocated to a fresh MS medium

devoid of Tunicamycin (Tm), allowing them to recover from the ER stress over another

three days. The total fresh weight of 10 plants, covering three biological replicates with

two technical replicates for each biological replicate, was documented.

Upon completion of the survival assay, chlorophyll was isolated using 100% methanol.

The levels were then quantified using a Tecan microplate reader at wavelengths of 652

nm for chlorophyll a and 665 nm for chlorophyll b.

Preparation of 35S::WT/M1/M2 bZIP60-GUS constructs:

DNA was extracted from 4-5 weeks old wild type Col-0 plants using 200 μl of

CTAB extraction buffer. This buffer was composed of 2% cetyl-trimethyl ammonium

bromide (CTAB), 100 mM Tris (pH 8.0), 20 mM EDTA (pH 8.0), 1.4 M NaCl, 0.5% β-

Mercaptoethanol, and 2% polyvinyl pyrrolidone. The Coding DNA (CD) region of

bZIP60 (spanning 888 base pairs) was amplified from the genomic DNA of the wild type

Col-0 using PCR. The amplification was carried out using Phusion Polymerase (Thermo

Scientific) and primers flanked by attB sites (Table S1). The PCR products were incorpo-

rated into the pDONR207 Gateway vector using BP reactions (Invitrogen). The entry

clones were then verified using PCR and Sanger sequencing, with the specific primers

outlined in Table S1. The pDONR207 vector was subsequently employed to introduce

nique of site-directed mutagenesis. The introduced mutations were verified using PCR and Sanger sequencing. Destination clones were assembled using LR reactions with the plant expression vector pMDC10 (C-GUS) (Addgene plasmid #118,492). These clones were then verified through PCR and Sanger sequencing. The resulting constructs, denoted as 2x35S::bZIP60 (WT/M1/M2)-GUS, were introduced into Agrobacterium tumefaciens (strain GV3101) to perform subsequent transient expression assays.

Quantitative and qualitative GUS assay:

Plants of different genotypes, aged between 4-5 weeks, were subjected to agroinfiltration using a needleless syringe, following a previously described article [126]. Three days after inoculation, the plant tissues were harvested and ground under the condition of liquid nitrogen. The total proteins were extracted from the collected tissue using an extraction buffer. This buffer was composed of 50 mM $NaPO_4$ (with a pH of 7.0), 1 mM Na_2EDTA, 0.1% SDS, 0.1% Triton X-100, a protease inhibitor meant for plant extracts (Sigma), and 10 mM β-mercaptoethanol, following a method described earlier [127]. After a centrifugation step (10 minutes at 4000×g and 4 °C), the supernatants were collected, and the protein concentration was determined using Bradford Reagent (Sigma). The proteins extracted were then incubated with 1 mM MUG (4-methylumbelliferyl β-D-glucuronide) to measure GUS activity. To halt the reaction, a stop buffer composed of 1 M Na_2CO_3 was used. The resulting fluorescence was quantified using a microplate reader (Tecan), using an excitation wavelength of 365 nm, an emission wavelength of 455 nm, and a filter wavelength of 430 nm. The relative MUG values were calculated by adjusting the

procedures was adapted from a previously published protocol [128].

For the histochemical assay, leaf tissues were harvested at 3 days post-inocula-tion. Following this, a staining solution was introduced into the leaves through vacuum infiltration. This staining solution was composed of 100 mM NaPO4 (with a pH of 7.0), 10 mM Na_2EDTA, 0.1% Triton X-100, 1 mM $K_3Fe(CN)_6$, 2 mM X-Gluc (50 mg/ml) in dimethylformamide (DMF) and nuclease-free water. Subsequently, the leaf tissues were immersed in the staining solution, covered with aluminum foil, and incubated at a tem-perature of 37°C for a duration of 24-48 hours. Following incubation, the leaves were re-moved from the staining solution and sequentially washed with increasing concentrations of ethanol (ranging from 30% to 80%) every hour to effectively eliminate the chloro-phyll. Then the pictures were taken using a scanner.

Bacterial strains and plant resistance quantification:

The bacterium _Pseudomonas syringae_ pv. tomato DC3000 (_Pst_ DC3000) was used for the pathogen infection and quantification assays. Soil grown 4-5 weeks old plants were infiltrated using a needleless syringe with _Pst_ DC3000 ($OD_{600} = 0.001$) to test the enhanced disease resistance (EDR). For each replication, three leaves per plant were used, with a total of six plants. At least three independent biological replicates were per-formed. Two days post-inoculation, bacterial growth was quantified following a previ-ously described protocol [94].

Plants that were grown in soil for a period of 4-5 weeks were infiltrated with *Pst* DC3000 avrRPM1 at (OD_{600} = 0.01). Using a needleless syringe, three leaves per plant were infiltrated for the procedure. Using a hole puncher, leaf discs were punched and promptly transferred into a beaker containing deionized water. Following a 30-minute period, the leaf discs were relocated into Falcon tubes, each containing 15ml of sterile deionized water per 15 leaf discs and the conductivity was then determined using a conductivity meter (Fisher, cat: 13-636-AP85) for every 30 minutes for 8 hours of post-inoculation.

Assay for measuring cell death through Caspase Assay:

To measure the caspase activity 4-5 weeks old plants were syringae infiltrated with *Pst* DC3000 avrRPM1 at (OD_{600} = 0.01). In the assay, three leaves per plant were used, with three plants per biological replication. At least three biological replications were performed in total. Leaf samples were collected eight- and 24-hours post-inoculation. The proteins were extracted from collected samples using a extraction buffer composed of: 50mM HEPES (pH 7.5), 5% glycerol, 1mM EDTA, 1mM DTT, 1mM PMSF, 0.1% triton and 50mM NaCl. The extracted proteins underwent centrifugation, after which the supernatants were collected and diluted using assay buffer. The diluted proteins were then combined with stock substrate buffer of synthetic caspases and incubated the plate at 30°C. Caspase activity was measured at 360nm excitation and 465nm emission using a plate reader. Protein concentrations were determined using a Bradford assay.

quantify the caspase-like activity.

Statistical analysis:

Statistical analysis was performed using one-way ANOVA and two-tailed t-test in either Excel or GraphPad Prism to determine significant differences. The graphs presented in Figures 1a, 2b, 2c, 2d, 2e, 3a, 3b, 3d, 4b and 4c were generated using GraphPad Prism. Statistically significant differences are denoted by asterisks: * for $p < 0.05$, ** for $p < 0.01$, *** for $p < 0.001$, and **** for $p < 0.0001$.

1   Zhang, W. *et al.* Plastic Transcriptomes Stabilize Immunity to Pathogen Diversity: The Jasmonic Acid and Salicylic Acid Networks within the Arabidopsis/Botrytis Pathosystem. *Plant Cell* **29**, 2727-2752, doi:10.1105/tpc.17.00348 (2017).

2   Jones, J. D. & Dangl, J. L. The plant immune system. *Nature* **444**, 323-329, doi:10.1038/nature05286 (2006).

3   Zipfel, C. & Felix, G. Plants and animals: a different taste for microbes? *Curr Opin Plant Biol* **8**, 353-360, doi:10.1016/j.pbi.2005.05.004 (2005).

4   Dangl, J. L. & Jones, J. D. Plant pathogens and integrated defence responses to infection. *Nature* **411**, 826-833, doi:10.1038/35081161 (2001).

5   Chisholm, S. T., Coaker, G., Day, B. & Staskawicz, B. J. Host-microbe interactions: shaping the evolution of the plant immune response. *Cell* **124**, 803-814, doi:10.1016/j.cell.2006.02.008 (2006).

6   Nimchuk, Z., Eulgem, T., Holt, B. F., 3rd & Dangl, J. L. Recognition and response in the plant immune system. *Annu Rev Genet* **37**, 579-609, doi:10.1146/annurev.genet.37.110801.142628 (2003).

7   Lam, E. Controlled cell death, plant survival and development. *Nat Rev Mol Cell Biol* **5**, 305-315, doi:10.1038/nrm1358 (2004).

8   Thomma, B. P., Nurnberger, T. & Joosten, M. H. Of PAMPs and effectors: the blurred PTI-ETI dichotomy. *Plant Cell* **23**, 4-15, doi:10.1105/tpc.110.082602 (2011).

9   Gust, A. A., Pruitt, R. & Nurnberger, T. Sensing Danger: Key to Activating Plant Immunity. *Trends Plant Sci* **22**, 779-791, doi:10.1016/j.tplants.2017.07.005 (2017).

10   Alvarez, M. E. Salicylic acid in the machinery of hypersensitive cell death and disease resistance. *Plant Mol Biol* **44**, 429-442, doi:10.1023/a:1026561029533 (2000).

11   Ding, P. & Ding, Y. Stories of Salicylic Acid: A Plant Defense Hormone. *Trends Plant Sci* **25**, 549-565, doi:10.1016/j.tplants.2020.01.004 (2020).

12   Chern, M. S. *et al.* Evidence for a disease-resistance pathway in rice similar to the NPR1-mediated signaling pathway in Arabidopsis. *Plant J* **27**, 101-113, doi:10.1046/j.1365-313x.2001.01070.x (2001).

13   Mou, Z., Fan, W. & Dong, X. Inducers of plant systemic acquired resistance regulate NPR1 function through redox changes. *Cell* **113**, 935-944, doi:10.1016/s0092-8674(03)00429-x (2003).

14   Pajerowska-Mukhtar, K. M., Emerine, D. K. & Mukhtar, M. S. Tell me more: roles of NPRs in plant immunity. *Trends Plant Sci* **18**, 402-411, doi:10.1016/j.tplants.2013.04.004 (2013).

15   Chen, J. *et al.* NPR1 Promotes Its Own and Target Gene Expression in Plant Defense by Recruiting CDK8. *Plant Physiol* **181**, 289-304, doi:10.1104/pp.19.00124 (2019).

Immunity Tradeoff. *Trends Plant Sci* **25**, 566-576, doi:10.1016/j.tplants.2020.02.002 (2020).

17   Fan, W. & Dong, X. In vivo interaction between NPR1 and transcription factor TGA2 leads to salicylic acid-mediated gene activation in Arabidopsis. *Plant Cell* **14**, 1377-1389, doi:10.1105/tpc.001628 (2002).

18   Afrin, T., Diwan, D., Sahawneh, K. & Pajerowska-Mukhtar, K. Multilevel regulation of endoplasmic reticulum stress responses in plants: where old roads and new paths meet. *J Exp Bot* **71**, 1659-1667, doi:10.1093/jxb/erz487 (2020).

19   Afrin, T., Seok, M., Terry, B. C. & Pajerowska-Mukhtar, K. M. Probing natural variation of IRE1 expression and endoplasmic reticulum stress responses in Arabidopsis accessions. *Sci Rep* **10**, 19154, doi:10.1038/s41598-020-76114-1 (2020).

20   Verchot, J. & Pajerowska-Mukhtar, K. M. UPR signaling at the nexus of plant viral, bacterial, and fungal defenses. *Curr Opin Virol* **47**, 9-17, doi:10.1016/j.coviro.2020.11.001 (2021).

21   Koizumi, N. *et al.* Molecular characterization of two Arabidopsis Ire1 homologs, endoplasmic reticulum-located transmembrane protein kinases. *Plant Physiol* **127**, 949-962 (2001).

22   Nagashima, Y. *et al.* Arabidopsis IRE1 catalyses unconventional splicing of bZIP60 mRNA to produce the active transcription factor. *Sci Rep* **1**, 29, doi:10.1038/srep00029 (2011).

23   Moreno, A. A. *et al.* IRE1/bZIP60-mediated unfolded protein response plays distinct roles in plant immunity and abiotic stress responses. *PLoS One* **7**, e31944, doi:10.1371/journal.pone.0031944 (2012).

24   Mishiba, K. *et al.* Defects in IRE1 enhance cell death and fail to degrade mRNAs encoding secretory pathway proteins in the Arabidopsis unfolded protein response. *Proc Natl Acad Sci U S A* **110**, 5713-5718, doi:10.1073/pnas.1219047110 (2013).

25   Iwata, Y., Fedoroff, N. V. & Koizumi, N. Arabidopsis bZIP60 is a proteolysis-activated transcription factor involved in the endoplasmic reticulum stress response. *Plant Cell* **20**, 3107-3121, doi:10.1105/tpc.108.061002 (2008).

26   Hollien, J. *et al.* Regulated Ire1-dependent decay of messenger RNAs in mammalian cells. *J Cell Biol* **186**, 323-331, doi:10.1083/jcb.200903014 (2009).

27   Urquiaga, M. C. O., Thiebaut, F., Hemerly, A. S. & Ferreira, P. C. G. From Trash to Luxury: The Potential Role of Plant LncRNA in DNA Methylation During Abiotic Stress. *Front Plant Sci* **11**, 603246, doi:10.3389/fpls.2020.603246 (2020).

28   Ponting, C. P., Oliver, P. L. & Reik, W. Evolution and functions of long noncoding RNAs. *Cell* **136**, 629-641, doi:10.1016/j.cell.2009.02.006 (2009).

29   Seo, J. S. *et al.* ELF18-INDUCED LONG-NONCODING RNA Associates with Mediator to Enhance Expression of Innate Immune Response Genes in Arabidopsis. *Plant Cell* **29**, 1024-1038, doi:10.1105/tpc.16.00886 (2017).

30   Xin, M. *et al.* Identification and characterization of wheat long non-protein

doi:10.1186/1471-2229-11-61 (2011).

31 Zhu, Q. H., Stephen, S., Taylor, J., Helliwell, C. A. & Wang, M. B. Long noncoding RNAs responsive to Fusarium oxysporum infection in Arabidopsis thaliana. *New Phytol* **201**, 574-584, doi:10.1111/nph.12537 (2014).

32 Wang, J. *et al.* Genome-wide analysis of tomato long non-coding RNAs and identification as endogenous target mimic for microRNA in response to TYLCV infection. *Sci Rep* **5**, 16946, doi:10.1038/srep16946 (2015).

33 Yu, Y. *et al.* Transcriptional landscape of pathogen-responsive lncRNAs in rice unveils the role of ALEX1 in jasmonate pathway and disease resistance. *Plant Biotechnol J* **18**, 679-690, doi:10.1111/pbi.13234 (2020).

34 Sun, Y., Zhang, H., Fan, M., He, Y. & Guo, P. Genome-wide identification of long non-coding RNAs and circular RNAs reveal their ceRNA networks in response to cucumber green mottle mosaic virus infection in watermelon. *Arch Virol* **165**, 1177-1190, doi:10.1007/s00705-020-04589-4 (2020).

35 Kumar, K. & Chakraborty, S. Roles of long non-coding RNAs in plant virus interactions. *Journal of Plant Biochemistry and Biotechnology* **30**, 684-697, doi:10.1007/s13562-021-00697-7 (2021).

36 Wang, H. *et al.* Genome-wide identification of long noncoding natural antisense transcripts and their responses to light in Arabidopsis. *Genome Res* **24**, 444-453, doi:10.1101/gr.165555.113 (2014).

37 He, Y., Vogelstein, B., Velculescu, V. E., Papadopoulos, N. & Kinzler, K. W. The antisense transcriptomes of human cells. *Science* **322**, 1855-1857 (2008).

38 Katayama, S. *et al.* Antisense transcription in the mammalian transcriptome. *Science* **309**, 1564-1566 (2005).

39 Oono, Y. *et al.* Genome-wide analysis of rice cis-natural antisense transcription under cadmium exposure using strand-specific RNA-Seq. *BMC Genomics* **18**, 761, doi:10.1186/s12864-017-4108-5 (2017).

40 Lu, T. *et al.* Strand-specific RNA-seq reveals widespread occurrence of novel cis-natural antisense transcripts in rice. *BMC Genomics* **13**, 721, doi:10.1186/1471-2164-13-721 (2012).

41 Liu, J. *et al.* Genome-wide analysis uncovers regulation of long intergenic noncoding RNAs in Arabidopsis. *Plant Cell* **24**, 4333-4345, doi:10.1105/tpc.112.102855 (2012).

42 Xu, J. *et al.* Natural antisense transcripts are significantly involved in regulation of drought stress in maize. *Nucleic Acids Res* **45**, 5126-5141, doi:10.1093/nar/gkx085 (2017).

43 Siegel, T. N. *et al.* Strand-specific RNA-Seq reveals widespread and developmentally regulated transcription of natural antisense transcripts in Plasmodium falciparum. *BMC Genomics* **15**, 150, doi:10.1186/1471-2164-15-150 (2014).

44 Yassour, M. *et al.* Strand-specific RNA sequencing reveals extensive regulated long antisense transcripts that are conserved across yeast species. *Genome Biol*

responsive nat-siRNAs in Brassica rapa. *BMC Plant Biol* **13**, 208, doi:10.1186/1471-2229-13-208 (2013).

46   Borsani, O., Zhu, J., Verslues, P. E., Sunkar, R. & Zhu, J. K. Endogenous siRNAs derived from a pair of natural cis-antisense transcripts regulate salt tolerance in Arabidopsis. *Cell* **123**, 1279-1291, doi:10.1016/j.cell.2005.11.035 (2005).

47   Sun, Q., Csorba, T., Skourti-Stathaki, K., Proudfoot, N. J. & Dean, C. R-loop stabilization represses antisense transcription at the Arabidopsis FLC locus. *Science* **340**, 619-621, doi:10.1126/science.1234848 (2013).

48   Marquardt, S. *et al.* Functional consequences of splicing of the antisense transcript COOLAIR on FLC transcription. *Mol Cell* **54**, 156-165, doi:10.1016/j.molcel.2014.03.026 (2014).

49   Jabnoune, M. *et al.* A rice cis-natural antisense RNA acts as a translational enhancer for its cognate mRNA and contributes to phosphate homeostasis and plant fitness. *The Plant Cell* **25**, 4166-4182 (2013).

50   Swiezewski, S., Liu, F., Magusin, A. & Dean, C. Cold-induced silencing by long antisense transcripts of an Arabidopsis Polycomb target. *Nature* **462**, 799-802, doi:10.1038/nature08618 (2009).

51   Wilusz, J. E., Sunwoo, H. & Spector, D. L. Long noncoding RNAs: functional surprises from the RNA world. *Genes Dev* **23**, 1494-1504, doi:10.1101/gad.1800909 (2009).

52   Faghihi, M. A. *et al.* Expression of a noncoding RNA is elevated in Alzheimer's disease and drives rapid feed-forward regulation of beta-secretase. *Nat Med* **14**, 723-730, doi:10.1038/nm1784 (2008).

53   Georg, J. *et al.* Evidence for a major role of antisense RNAs in cyanobacterial gene regulation. *Mol Syst Biol* **5**, 305, doi:10.1038/msb.2009.63 (2009).

54   Lewis, A. *et al.* Imprinting on distal chromosome 7 in the placenta involves repressive histone methylation independent of DNA methylation. *Nat Genet* **36**, 1291-1295, doi:10.1038/ng1468 (2004).

55   Zhao, X. *et al.* Global identification of Arabidopsis lncRNAs reveals the regulation of MAF4 by a natural antisense RNA. *Nat Commun* **9**, 5056, doi:10.1038/s41467-018-07500-7 (2018).

56   Deforges, J. *et al.* Control of Cognate Sense mRNA Translation by cis-Natural Antisense RNAs. *Plant Physiol* **180**, 305-322, doi:10.1104/pp.19.00043 (2019).

57   Prescott, E. M. & Proudfoot, N. J. Transcriptional collision between convergent genes in budding yeast. *Proc Natl Acad Sci U S A* **99**, 8796-8801, doi:10.1073/pnas.132270899 (2002).

58   Katiyar-Agarwal, S. *et al.* A pathogen-inducible endogenous siRNA in plant immunity. *Proc Natl Acad Sci U S A* **103**, 18002-18007, doi:10.1073/pnas.0608258103 (2006).

59   Hastings, M. L., Milcarek, C., Martincic, K., Peterson, M. L. & Munroe, S. H. Expression of the thyroid hormone receptor gene, erbAalpha, in B lymphocytes: alternative mRNA processing is independent of differentiation but correlates

doi:10.1093/nar/25.21.4296 (1997).

60   Peters, N. T., Rohrbach, J. A., Zalewski, B. A., Byrkett, C. M. & Vaughn, J. C. RNA editing and regulation of Drosophila 4f-rnp expression by sas-10 antisense readthrough mRNA transcripts. *RNA* **9**, 698-710, doi:10.1261/rna.2120703 (2003).

61   Okamoto, M. *et al.* Genome-wide analysis of endogenous abscisic acid-mediated transcription in dry and imbibed seeds of Arabidopsis using tiling arrays. *Plant J* **62**, 39-51, doi:10.1111/j.1365-313X.2010.04135.x (2010).

62   Fedak, H. *et al.* Control of seed dormancy in Arabidopsis by a cis-acting noncoding antisense transcript. *Proc Natl Acad Sci U S A* **113**, E7846-E7855, doi:10.1073/pnas.1608827113 (2016).

63   Csorba, T., Questa, J. I., Sun, Q. & Dean, C. Antisense COOLAIR mediates the coordinated switching of chromatin states at FLC during vernalization. *Proc Natl Acad Sci U S A* **111**, 16160-16165, doi:10.1073/pnas.1419030111 (2014).

64   Wunderlich, M., Gross-Hardt, R. & Schoffl, F. Heat shock factor HSFB2a involved in gametophyte development of Arabidopsis thaliana and its expression is controlled by a heat-inducible long non-coding antisense RNA. *Plant Mol Biol* **85**, 541-550, doi:10.1007/s11103-014-0202-0 (2014).

65   Kindgren, P., Ard, R., Ivanov, M. & Marquardt, S. Transcriptional read-through of the long non-coding RNA SVALKA governs plant cold acclimation. *Nat Commun* **9**, 4561, doi:10.1038/s41467-018-07010-6 (2018).

66   Liu, X. *et al.* A novel antisense long noncoding RNA, TWISTED LEAF, maintains leaf blade flattening by regulating its associated sense R2R3-MYB gene in rice. *New Phytol* **218**, 774-788, doi:10.1111/nph.15023 (2018).

67   Cui, J., Luan, Y., Jiang, N., Bao, H. & Meng, J. Comparative transcriptome analysis between resistant and susceptible tomato allows the identification of lncRNA16397 conferring resistance to Phytophthora infestans by co-expressing glutaredoxin. *Plant J* **89**, 577-589, doi:10.1111/tpj.13408 (2017).

68   Lu, C. *et al.* Genome-wide analysis for discovery of rice microRNAs reveals natural antisense microRNAs (nat-miRNAs). *Proc Natl Acad Sci U S A* **105**, 4951-4956, doi:10.1073/pnas.0708743105 (2008).

69   Ha, M. & Kim, V. N. Regulation of microRNA biogenesis. *Nat Rev Mol Cell Biol* **15**, 509-524, doi:10.1038/nrm3838 (2014).

70   Broughton, J. P., Lovci, M. T., Huang, J. L., Yeo, G. W. & Pasquinelli, A. E. Pairing beyond the Seed Supports MicroRNA Targeting Specificity. *Mol Cell* **64**, 320-333, doi:10.1016/j.molcel.2016.09.004 (2016).

71   Vasudevan, S. Posttranscriptional upregulation by microRNAs. *Wiley Interdiscip Rev RNA* **3**, 311-330, doi:10.1002/wrna.121 (2012).

72   Makarova, J. A. *et al.* Intracellular and extracellular microRNA: An update on localization and biological role. *Prog Histochem Cytochem* **51**, 33-49, doi:10.1016/j.proghi.2016.06.001 (2016).

journey for small RNAs. *Genome Biol* **12**, 215, doi:10.1186/gb-2010-11-12-219 (2011).

74   Li, S. *et al.* Unidirectional movement of small RNAs from shoots to roots in interspecific heterografts. *Nat Plants* **7**, 50-59, doi:10.1038/s41477-020-00829-2 (2021).

75   Zhang, T. *et al.* Cotton plants export microRNAs to inhibit virulence gene expression in a fungal pathogen. *Nat Plants* **2**, 16153, doi:10.1038/nplants.2016.153 (2016).

76   Betti, F. *et al.* Exogenous miRNAs induce post-transcriptional gene silencing in plants. *Nat Plants* **7**, 1379-1388, doi:10.1038/s41477-021-01005-w (2021).

77   Wang, J. W. *et al.* Control of root cap formation by MicroRNA-targeted auxin response factors in Arabidopsis. *Plant Cell* **17**, 2204-2216, doi:10.1105/tpc.105.033076 (2005).

78   Guo, H. S., Xie, Q., Fei, J. F. & Chua, N. H. MicroRNA directs mRNA cleavage of the transcription factor NAC1 to downregulate auxin signals for arabidopsis lateral root development. *Plant Cell* **17**, 1376-1386, doi:10.1105/tpc.105.030841 (2005).

79   Varallyay, E., Valoczi, A., Agyi, A., Burgyan, J. & Havelda, Z. Plant virus-mediated induction of miR168 is associated with repression of ARGONAUTE1 accumulation. *EMBO J* **29**, 3507-3519, doi:10.1038/emboj.2010.215 (2010).

80   Hajdarpasic, A. & Ruggenthaler, P. Analysis of miRNA expression under stress in Arabidopsis thaliana. *Bosn J Basic Med Sci* **12**, 169-176, doi:10.17305/bjbms.2012.2471 (2012).

81   Phillips, J. R., Dalmay, T. & Bartels, D. The role of small RNAs in abiotic stress. *FEBS Lett* **581**, 3592-3597, doi:10.1016/j.febslet.2007.04.007 (2007).

82   Zhang, B. MicroRNA: a new target for improving plant tolerance to abiotic stress. *J Exp Bot* **66**, 1749-1761, doi:10.1093/jxb/erv013 (2015).

83   Gao, P. *et al.* Over-expression of osa-MIR396c decreases salt and alkali stress tolerance. *Planta* **231**, 991-1001, doi:10.1007/s00425-010-1104-2 (2010).

84   Song, J. B. *et al.* miR394 and LCR are involved in Arabidopsis salt and drought stress responses in an abscisic acid-dependent manner. *BMC Plant Biol* **13**, 210, doi:10.1186/1471-2229-13-210 (2013).

85   Xie, F., Jones, D. C., Wang, Q., Sun, R. & Zhang, B. Small RNA sequencing identifies miRNA roles in ovule and fibre development. *Plant Biotechnol J* **13**, 355-369, doi:10.1111/pbi.12296 (2015).

86   Guan, X. *et al.* miR828 and miR858 regulate homoeologous MYB2 gene functions in Arabidopsis trichome and cotton fibre development. *Nat Commun* **5**, 3050, doi:10.1038/ncomms4050 (2014).

87   Chitnis, N. S. *et al.* miR-211 is a prosurvival microRNA that regulates chop expression in a PERK-dependent manner. *Mol Cell* **48**, 353-364, doi:10.1016/j.molcel.2012.08.025 (2012).

88   Duan, Q. *et al.* ER stress negatively modulates the expression of the miR-199a/214 cluster to regulates tumor survival and progression in human

(2012).

89   Byrd, A. E., Aragon, I. V. & Brewer, J. W. MicroRNA-30c-2* limits expression of proadaptive factor XBP1 in the unfolded protein response. *J Cell Biol* **196**, 689-698, doi:10.1083/jcb.201201077 (2012).

90   Bartoszewska, S., Cabaj, A., Dabrowski, M., Collawn, J. F. & Bartoszewski, R. miR-34c-5p modulates X-box-binding protein 1 (XBP1) expression during the adaptive phase of the unfolded protein response. *FASEB J* **33**, 11541-11554, doi:10.1096/fj.201900600RR (2019).

91   Li, M. *et al.* Upregulation of miR-665 promotes apoptosis and colitis in inflammatory bowel disease by repressing the endoplasmic reticulum stress components XBP1 and ORMDL3. *Cell Death Dis* **8**, e2699, doi:10.1038/cddis.2017.76 (2017).

92   Maurel, M., Dejeans, N., Taouji, S., Chevet, E. & Grosset, C. F. MicroRNA-1291-mediated silencing of IRE1alpha enhances Glypican-3 expression. *RNA* **19**, 778-788, doi:10.1261/rna.036483.112 (2013).

93   McCormack, M. E., Liu, X., Jordan, M. R. & Pajerowska-Mukhtar, K. M. An improved high-throughput screening assay for tunicamycin sensitivity in Arabidopsis seedlings. *Frontiers in Plant Science* **6**, 663 (2015).

94   Liu, X. *et al.* Bacterial Leaf Infiltration Assay for Fine Characterization of Plant Defense Responses using the Arabidopsis thaliana-Pseudomonas syringae Pathosystem. *J Vis Exp*, doi:10.3791/53364 (2015).

95   Lam, E. & Pozo, O. d. Caspase-like protease involvement in the control of plant cell death. *Plant molecular biology* **44**, 417-428 (2000).

96   Woltering, E. J. Death proteases come alive. *Trends in plant science* **9**, 469-472 (2004).

97   Zuppini, A., Navazio, L. & Mariani, P. Endoplasmic reticulum stress-induced programmed cell death in soybean cells. *Journal of cell science* **117**, 2591-2598 (2004).

98   Cui, F. *et al.* Ectopic expression of BOTRYTIS SUSCEPTIBLE1 reveals its function as a positive regulator of wound-induced cell death and plant susceptibility to Botrytis. *The Plant Cell* **34**, 4105-4116, doi:10.1093/plcell/koac206 (2022).

99   Mengiste, T., Chen, X., Salmeron, J. & Dietrich, R. The BOTRYTIS SUSCEPTIBLE1 Gene Encodes an R2R3MYB Transcription Factor Protein That Is Required for Biotic and Abiotic Stress Responses in Arabidopsis. *The Plant Cell* **15**, 2551-2565, doi:10.1105/tpc.014167 (2003).

100   Cui, F., Brosche, M., Sipari, N., Tang, S. & Overmyer, K. Regulation of ABA dependent wound induced spreading cell death by MYB108. *New Phytol* **200**, 634-640, doi:10.1111/nph.12456 (2013).

101   Bahieldin, A. *et al.* Ethylene responsive transcription factor ERF109 retards PCD and improves salt tolerance in plant. *BMC Plant Biol* **16**, 216, doi:10.1186/s12870-016-0908-z (2016).

102   Bahieldin, A. *et al.* Multifunctional activities of ERF109 as affected by salt stress

Biol **64**, 477-499, doi:10.1146/annurev-arplant-050312-120053 (2013).

104   Mesitov, M. V. *et al.* Differential processing of small RNAs during endoplasmic reticulum stress. *Sci Rep* **7**, 46080, doi:10.1038/srep46080 (2017).

105   Pani, A., Mahapatra, R. K., Behera, N. & Naik, P. K. Computational identification of sweet wormwood (Artemisia annua) microRNA and their mRNA targets. *Genomics Proteomics Bioinformatics* **9**, 200-210, doi:10.1016/S1672-0229(11)60023-5 (2011).

106   Kim, J. H., Oh, T. R., Cho, S. K., Yang, S. W. & Kim, W. T. Inverse Correlation Between MPSR1 E3 Ubiquitin Ligase and HSP90.1 Balances Cytoplasmic Protein Quality Control. *Plant Physiol* **180**, 1230-1240, doi:10.1104/pp.18.01582 (2019).

107   Abdel-Ghany, S. E. & Pilon, M. MicroRNA-mediated systemic down-regulation of copper protein expression in response to low copper availability in Arabidopsis. *Journal of Biological Chemistry* **283**, 15932-15945 (2008).

108   Feng, Y. Z. *et al.* A Natural Variant of miR397 Mediates a Feedback Loop in Circadian Rhythm. *Plant Physiol* **182**, 204-214, doi:10.1104/pp.19.00710 (2020).

109   Zhang, Y. C. *et al.* Overexpression of microRNA OsmiR397 improves rice yield by increasing grain size and promoting panicle branching. *Nat Biotechnol* **31**, 848-852, doi:10.1038/nbt.2646 (2013).

110   Wang, C. Y. *et al.* MiR397b regulates both lignin content and seed number in Arabidopsis via modulating a laccase involved in lignin biosynthesis. *Plant Biotechnol J* **12**, 1132-1142, doi:10.1111/pbi.12222 (2014).

111   Hajieghrari, B., Farrokhi, N., Goliaei, B. & Kavousi, K. Computational identification of MicroRNAs and their transcript target (s) in field mustard (Brassica rapa L.). *Iranian Journal of Biotechnology* **15**, 22 (2017).

112   Kapadia, C. *et al.* Genome-Wide Identification, Quantification, and Validation of Differentially Expressed miRNAs in Eggplant (Solanum melongena L.) Based on Their Response to Ralstonia solanacearum Infection. *ACS Omega* **8**, 2648-2657, doi:10.1021/acsomega.2c07097 (2023).

113   Breakfield, N. W. *et al.* High-resolution experimental and computational profiling of tissue-specific known and novel miRNAs in Arabidopsis. *Genome Res* **22**, 163-176, doi:10.1101/gr.123547.111 (2012).

114   Selvaraj, G., Kumar, A., Jakse, J. & Matousek, J. Computational Prediction, Target Identification and Experimental Validation of miRNAs from Expressed Sequence Tags in Cannabis sativa. L. *Research & Reviews: Journal of BotanicalSciences* (2015).

115   Yang, G. *et al.* MicroRNAs transcriptionally regulate promoter activity in Arabidopsis thaliana. *J Integr Plant Biol* **61**, 1128-1133, doi:10.1111/jipb.12775 (2019).

116   Werner, A. & Sayer, J. A. Naturally occurring antisense RNA: function and mechanisms of action. *Curr Opin Nephrol Hypertens* **18**, 343-349, doi:10.1097/MNH.0b013e32832cb982 (2009).

117   Morris, K. V. & Mattick, J. S. The rise of regulatory RNA. *Nat Rev Genet* **15**, 423-

mutated cyclic nucleotide-gated ion channel. *Proc Natl Acad Sci U S A* **97**, 9323-9328, doi:10.1073/pnas.150005697 (2000).

119   Devoto, A. *et al.* Topology, subcellular localization, and sequence diversity of the Mlo family in plants. *J Biol Chem* **274**, 34993-35004, doi:10.1074/jbc.274.49.34993 (1999).

120   Clarke, A., Desikan, R., Hurst, R. D., Hancock, J. T. & Neill, S. J. NO way back: nitric oxide and programmed cell death in Arabidopsis thaliana suspension cultures. *Plant J* **24**, 667-677, doi:10.1046/j.1365-313x.2000.00911.x (2000).

121   Mittler, R., Shulaev, V. & Lam, E. Coordinated Activation of Programmed Cell Death and Defense Mechanisms in Transgenic Tobacco Plants Expressing a Bacterial Proton Pump. *Plant Cell* **7**, 29-42, doi:10.1105/tpc.7.1.29 (1995).

122   Bonneau, L., Ge, Y., Drury, G. E. & Gallois, P. What happened to plant caspases? *Journal of experimental botany* **59**, 491-499 (2008).

123   Sueldo, D. J. & van der Hoorn, R. A. L. Plant life needs cell death, but does plant cell death need Cys proteases? *FEBS J* **284**, 1577-1585, doi:10.1111/febs.14034 (2017).

124   Liu, X., Afrin, T. & Pajerowska-Mukhtar, K. M. Arabidopsis GCN2 kinase contributes to ABA homeostasis and stomatal immunity. *Commun Biol* **2**, 302, doi:10.1038/s42003-019-0544-x (2019).

125   Chen, C. *et al.* Real-time quantification of microRNAs by stem–loop RT–PCR. *Nucleic Acids Research* **33**, e179-e179, doi:10.1093/nar/gni178 (2005).

126   Mangano, S., Gonzalez, C. D. & Petruccelli, S. Agrobacterium tumefaciens-mediated transient transformation of Arabidopsis thaliana leaves. *Arabidopsis Protocols*, 165-173 (2014).

127   Pajerowska-Mukhtar, K. M. *et al.* The HSF-like transcription factor TBF1 is a major molecular switch for plant growth-to-defense transition. *Current Biology* **22**, 103-112 (2012).

128   Jefferson, R. A., Kavanagh, T. A. & Bevan, M. W. GUS fusions: beta-glucuronidase as a sensitive and versatile gene fusion marker in higher plants. *The EMBO journal* **6**, 3901-3907 (1987).